


High-spatiotemporal-resolution transcriptomes provide insights into fruit development and ripening in *Citrus sinensis*

Guizhi Feng[†], Juxun Wu[†] , Yanhui Xu, Liqing Lu and Hualin Yi*

Key Laboratory of Horticultural Plant Biology, Ministry of Education, Huazhong Agricultural University, Wuhan, China

Received 13 March 2019;

revised 30 December 2020;

accepted 7 January 2021.

*Correspondence (Tel +86 027 87284008;

fax +86 027 87282010;

email yihualin@mail.hzau.edu.cn)

[†]These authors contributed equally to the article.

Summary

Citrus fruit has a unique structure with soft leathery peel and pulp containing vascular bundles and several segments with many juice sacs. The function and morphology of each fruit tissue are different. Therefore, analysis at the organ-wide or mixed-tissue level inevitably obscures many tissue-specific phenomena. High-throughput RNA sequencing was used to profile *Citrus sinensis* fruit development based on four fruit tissue types and six development stages from young fruits to ripe fruits. Using a coexpression network analysis, modules of coexpressed genes and hub genes of tissue-specific networks were identified. Of particular importance is the discovery of the regulatory network of phytohormones during citrus fruit development and ripening. A model was proposed to illustrate how *ABF2* mediates the ABA signalling involved in sucrose transport, chlorophyll degradation, auxin homeostasis, carotenoid and ABA biosynthesis, and cell wall metabolism during citrus fruit development. Moreover, we depicted the detailed spatiotemporal expression patterns of the genes involved in sucrose and citric acid metabolism in citrus fruit and identified several key genes that may play crucial roles in sucrose and citric acid accumulation in the juice sac, such as *SWEET15* and *CsPH8*. The high spatial and temporal resolution of our data provides important insights into the molecular networks underlying citrus fruit development and ripening.

Keywords: Citrus fruit, ABA, auxin, transcriptome, sucrose transporter, citric acid metabolism.

Introduction

Fruits are generally morphologically classified into silique (e.g. *Arabidopsis*), berry (e.g. tomato), pome (e.g. pear) and hesperidium (e.g. citrus) types among others. The mechanisms underlying fruit development and ripening are unique among different fruit types (Ding *et al.*, 2015). Citrus fruits are classified as hesperidium and have non-climacteric fruit maturation characteristics (Paul *et al.*, 2012). The development and ripening of citrus fruits can be divided into three stages: cell division stage; expansion stage, which involves cell enlargement, water accumulation, and sugar accumulation; and ripening stage (Bain, 1958). At the ripening stage, pigments, sugars and other soluble solids are accumulated, chlorophyll and organic acid are reduced, and the cell wall is extensively modified (Katz *et al.*, 2011; Yu *et al.*, 2012).

Understanding the hormonal regulation of citrus fruit development and ripening is of considerable academic and agronomic value. Previous studies showed that auxin plays a pivotal role in the regulation of fruit set and growth (Goetz *et al.*, 2007; de Jong *et al.*, 2009; Kang *et al.*, 2013; Pattison *et al.*, 2015). The strict spatiotemporal control of auxin distribution and signalling during fruit development was discovered in *Arabidopsis* (Sundberg and Ostergaard, 2009), tomato (Pattison *et al.*, 2014) and strawberry (Kang *et al.*, 2013). However, a comprehensive investigation of tissue-specific, auxin-related gene expression to illustrate the action of auxin in citrus fruit is currently lacking. The ripening mechanisms of climacteric fruits, especially the mechanism related to ethylene (ETH), have been well studied (Alexander

and Grierson, 2002; Klee and Giovannoni, 2011). However, the mechanisms underlying the ripening of non-climacteric fruits remain unclear. Absciscic acid (ABA) was considered to be a ripening control factor for non-climacteric fruits. The levels of ABA sharply increased during the onset of fruit ripening and/or ripening processes in citrus (Wu *et al.*, 2014b), strawberry (Jia *et al.*, 2011) and cucumber (Wang *et al.*, 2012). The peak ABA level of a late-ripening sweet orange mutant was obtained later than that of the wild-type fruit (Wu *et al.*, 2014b). Similarly, the degreening stage was delayed in a fruit-specific ABA-deficient mutant of sweet orange (Rodrigo *et al.*, 2003; Romero *et al.*, 2012). Moreover, ABA promoted fruit ripening and played an important role in the regulation of fruit development and ripening in strawberry (Ji *et al.*, 2012; Jia *et al.*, 2011; Jia *et al.*, 2013) and cucumber (Wang *et al.*, 2013). Although considerable progress has been made in describing the role of ABA in the regulation of fleshy fruit ripening, the molecular mechanisms remain to be elucidated. To uncover the mechanisms of ABA action at the molecular level, it is necessary to identify all of the components involved in ABA homeostasis, spatiotemporal distribution and regulatory network.

Sucrose directly accumulates in citrus fruit and is stored in the vacuoles of juice sacs (JSs) cells and mainly translocated from leaves (Sadka *et al.*, 2019). The sugar post-phloem transport is the rate-limiting step (Koch and Avigne, 1990). In citrus fruit, apoplastic and symplastic pathways both occur in post-phloem transport (Koch *et al.*, 1986; Nli and Coombe, 1988). In the apoplastic pathway, sugar transport is dependent on transport

proteins, including SUTs, SWEETs and TMTs. SWEET proteins function in the efflux of sucrose to the apoplast (Chen *et al.*, 2012). The plasma membrane SUT sucrose/proton cotransporters and TMT sucrose/proton antiporters function in transporting sugar into the cytoplasm and vacuole, respectively (Schneider *et al.*, 2012; Schulz *et al.*, 2011). In citrus, sucrose is delivered to the fruit by the funicular phloem, which is connected to the segment epidermis. Following phloem unloading, sucrose moves into the segment epidermis and parenchymatous, which are hair-like stalks of individual JSs (Koch, 1983; Koch and Avigne, 1990). However, the molecular mechanism underlying sucrose transport into JS cells remains unclear.

Acidity is important for fruit taste. In citrus, acidity is generally dependent on citrate accumulation in the vacuole of JS cells, where citrate contributes more than 90% of the total organic acids. Citrate accumulation in the vacuole depends on the balance of citrate synthesis, transport and degradation or utilization (Cercos *et al.*, 2006a; Sadka *et al.*, 2000). Previous studies (Aprile *et al.*, 2011; Muller and Taiz, 2002; Shi *et al.*, 2015) indicated that vacuolar-type and p-type ATPases play important roles in citrate uptake into the vacuole, the citrate/H⁺ symporter Cscit1 (Shimada *et al.*, 2006) mediates citrate efflux from the vacuole into the cytoplasm, and citrate is utilized through the Aco-GABA and/or ACL-degradation pathways (Cercos *et al.*, 2006b; Guo *et al.*, 2016; Hu *et al.*, 2015).

Generally, seedless citrus fruit can be divided into four tissues: epicarp (EP; referred to as the flavedo), albedo (AL; the spongy white part of the peel), segment membrane (SM; referred to as the segment epidermis, which covers the carpel and JS) and JS (stores a large number of nutritional components beneficial to health) (Sadka *et al.*, 2019). In this study, we chose a navel orange variety (seedless) 'Fengjie 72-1' (*Citrus sinensis*) as the research material, and the EP, AL, SM and JS tissues of this variety can be easily obtained via manual dissection. The fruits were sampled at six stages beginning at 50 days after flowering (DAF) until 220 DAF, which covered the fruit development and ripening periods. Using second-generation sequencing technology, we profiled whole-stage fruit transcriptomes of *C. sinensis* and produced high-resolution profiles of the global gene expression in four different fruit tissues at six developmental stages. Overall, this study aimed to uncover new molecular insights into citrus fruit development and ripening and to reveal the specific non-climacteric characteristics of citrus fruit.

Results

Global analysis of the transcriptomes of dissected fruit tissues

To uncover the underlying molecular network that regulates citrus fruit development and ripening, we used RNA-seq to quantify the transcriptomes of 24 fruit tissue samples, including four tissue types at six developmental stages (50–220 DAF; Figure 1a; Table S1). The fruits were sampled after the second physiological fruit-falling period (50 DAF), during the expansion period (80, 120 and 155 DAF), at the colouring period (180 DAF) and at the full-ripening period (220 DAF). The correlation dendrogram illustrates the global relative relationships among the 24 tissues (Figure 1b). All three biological replicates of each sample clustered together, with the exception of AL_2_1 and AL_3_1. The EP samples were clustered together (Figure 1b). For the AL, SM and JS tissues, the following samples were clustered together: stages 1 and 2; stages 3 and 4; stages 5 and 6

(Figure 1b). At stages 1 and 2, the differences among the tissues were less than the differences between the stages, while at stage 3 to stage 6, the differences among the tissues were larger than those between the two stages (Figure 1b).

Normalized read counts (fragments per kilobase of transcript sequence per million base pairs sequenced, FPKM) for each gene were calculated. Between 16 621 (JS6) and 19 455 (EP1) genes with FPKM values more than 0.3 remained in each sample, and more than 85% of which were in the 1 to 100 FPKM range (Figure 1c; Table S2). The genes from all six stages of the same tissue were combined, and a Venn diagram was used to reveal unique or commonly expressed genes among the fruit tissues (Figure 1d). A total of 18 156 genes were common among all four fruit tissues. Notably, of the four tissues, the EP had the largest number of tissue-specific genes.

To identify different gene expression profiles across citrus fruit development in each tissue, STEM (Short Time-series Expression Miner; Ernst and Bar-Joseph, 2006) was used to perform clustering. The results showed that 11, 13, 11 and 7 statistically significant model profiles (coloured profiles) were identified in EP, AL, SM and JS, respectively (Figure 2a; Table S3). In these four tissues, two special model profiles (profile 8, down-regulated profile; profile 39, up-regulated profile) were identified (Figure 2a). Venn diagrams revealed that the number of unique expressed genes was more than that of commonly expressed genes among the four fruit tissues in both profile 39 and profile 8 (Figure 2b), suggesting that different regulation networks occur in each fruit tissue during fruit development. A similar result was also revealed in the Gene Ontology (GO) term enrichment analysis (Figure S1; Table S4). In addition, the eight gene sets of profile 8 and profile 39 were subjected to a pathway enrichment analysis (Table S5). As shown in Figure 2c, more genes associated in the citrate cycle, proteasome, pyruvate metabolism and carotenoid biosynthesis pathways were up-regulated than down-regulated. Notably, in profile 39_JS, the prevalence of enriched genes in the citrate cycle pathway reached 51% (23/45) of all citrate cycle pathway genes, indicating that the TCA cycle was continuously enhanced in JS with citrus fruit development.

Coexpression network analysis reveals distinct regulatory programmes among *C. sinensis* fruit tissue development

To reveal the functions of networks instead of individual genes, the system biology approach weighted gene coexpression network analysis (WGCNA) (Langfelder and Horvath, 2008) was used to construct coexpression networks. This analysis resulted in 15 distinct modules and one module in grey colour reserved for genes outside of all modules (Figure S2; Table S6). Three tissue-specific modules (blue, 2462 genes; purple, 313 genes; and black, 442 genes) were further analysed (Figure 3a, d and g). The three gene sets of the blue, purple and black modules were subjected to a GO term enrichment analysis (Figure 3b, e and h; Table S7). The genes coexpressed in the blue module (the EP-specific module) were significantly enriched in the 'lipid metabolism', 'response to cadmium ion' and 'flavonoid metabolism' biological processes (Figure 3b). In the purple module (the AL- and SM-specific module), genes were significantly enriched in the 'phloem or xylem histogenesis', 'transport' and 'response to toxic substance' biological processes (Figure 3e). The genes of the black module (the SM- and JS-specific module) were mainly involved in the 'translation', 'ribosome biogenesis' and 'protein transport' biological processes (Figure 3h). To further identify the key

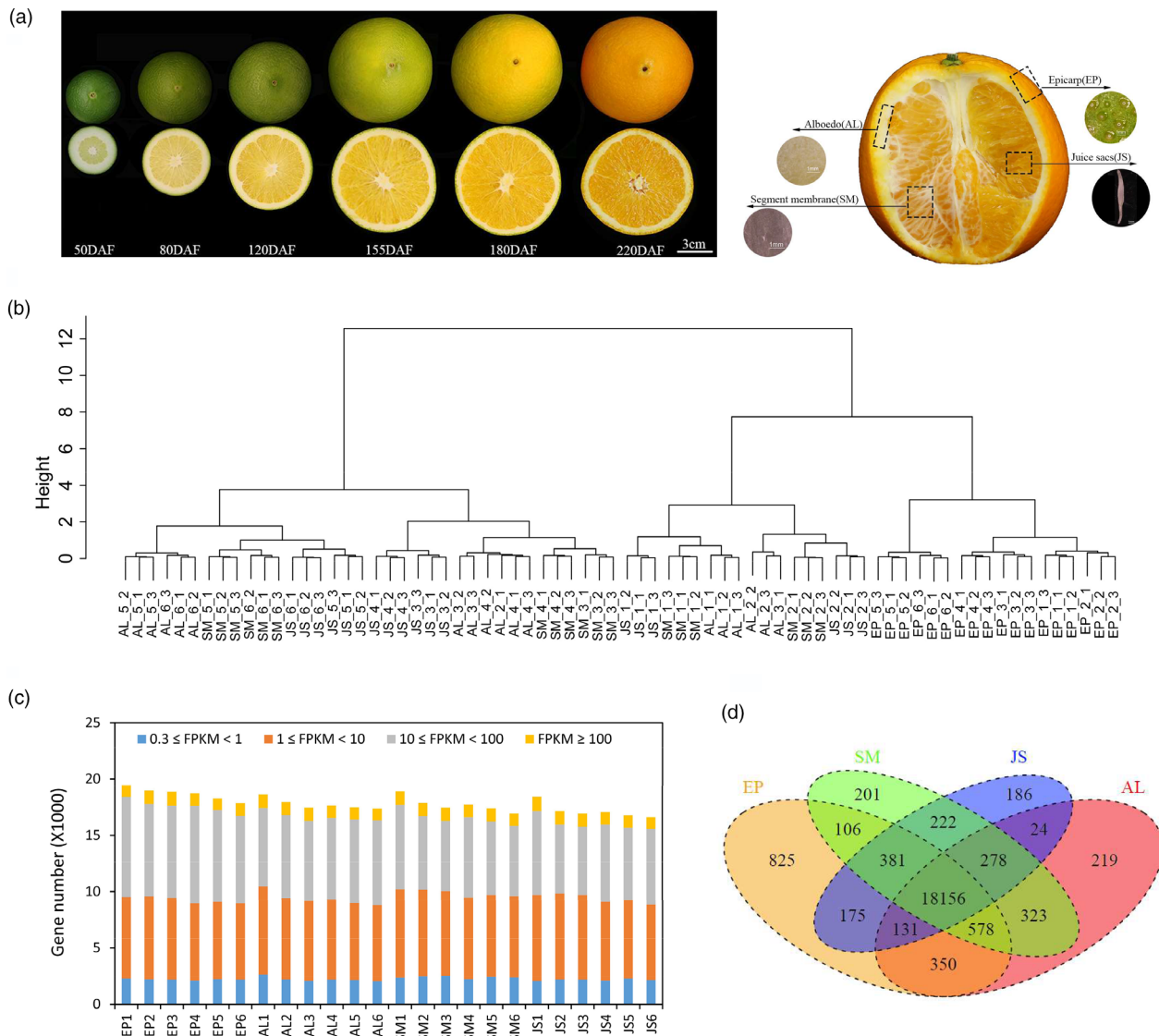


Figure 1 Fruit tissue collection and global analysis of the fruit transcriptomes. (a) Six stages of *C. sinensis* fruit development and four fruit tissue types, epicarp, albedo, segment membrane and juice sac, collected for RNA-seq. (b) Cluster dendrogram showing the global relationships between biological replicates and among different stages and tissues. The y-axis is the degree of variance. In the following figures, samples are named 'Tissue_stage_replicate'; 'EP_2_1' represent 'Epicarp_Stage 2_Replicate 1'. (c) Number of genes expressed in each tissue with an average FPKM higher than 0.3. (d) Venn diagram showing the number of shared and uniquely expressed genes among the four fruit tissues.

regulatory genes in these modules, WGCNA and Cytoscape (Shannon *et al.*, 2003) were employed to construct and visualize gene networks, in which each node represented a gene and the connecting lines (edges) between genes represented coexpression correlations. The hub genes, which have the most connections in the network, may be the key regulatory genes. In the blue, purple and black module networks, 20 of 512 genes, 18 of 152 genes, and 12 of 134 genes encoded transcription factors (TFs), respectively (Figure 3c, f and i; Table S8). For instance, *CsAPL* (orange1.1t03247) is the hub gene with the highest number of edges (98 edges) in the purple module network (Figure 3f). In other module networks, the highly connected hub TFs included *CsKAN2* (Cs3g09270), *CsERF13* (Cs1g03290), *CsMYB5* (Cs9g03070), and *CsTT8* (Cs5g31400). (Figure 3c, f and i).

In previous studies (Karlova *et al.*, 2014; Leng *et al.*, 2014; Zhang *et al.*, 2015), ABA, jasmonic acid (JA) and indole-3-acetic acid (IAA) were shown to play important roles in fruit development and ripening. We measured the ABA, IAA and JA contents in each fruit tissue across the six developmental stages (Figure 5a, c and e). The associations among modules and plant hormones were determined via the WGCNA. As shown in Figure 4a, ABA was highly correlated with the green module ($r^2 = 0.74$, $P = 3e-05$) and JA was highly correlated with the yellow module ($r^2 = 0.88$, $P = 1e-08$). None of the modules were highly correlated with IAA. The genes coexpressed in the green module were significantly enriched in 'cellular macromolecule catabolism', 'response to osmotic stress' and 'intracellular transport' (Figure 4b, c; Table S7). In the yellow module, the genes were significantly enriched in 'response to wounding', 'organic

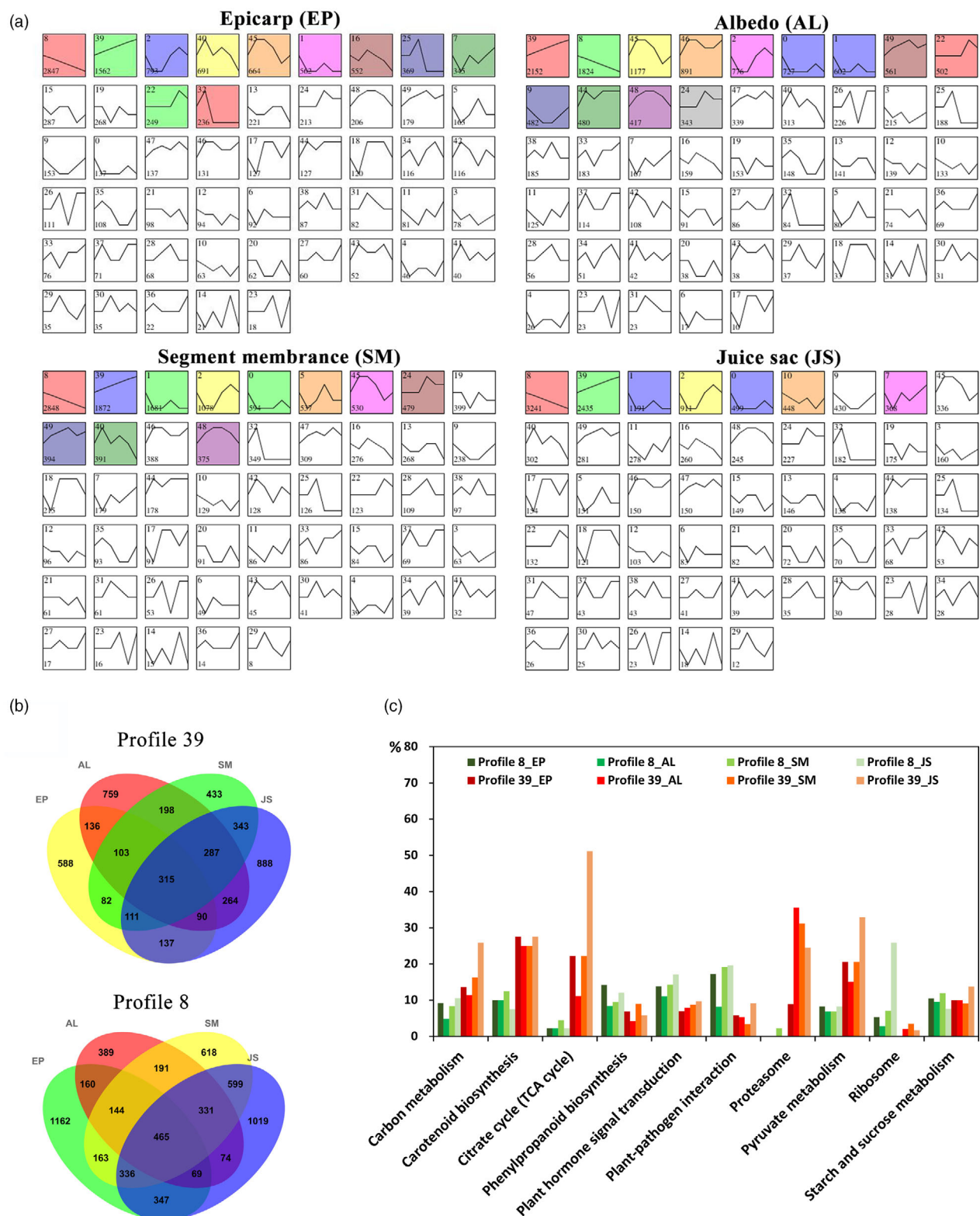


Figure 2 Gene expression profile analysis and functional enrichment analysis in each fruit tissue. (a) Module profiles of the genes in each fruit tissue across six developmental stages. (b) Venn diagrams showing the number of shared and uniquely expressed genes among the four fruit tissues in profiles 8 and 39. (c) KEGG pathway enrichment analysis results for the genes clustered in profiles 8 and 39 among the four fruit tissues. The x-axis represents the pathways, and the y-axis represents the percentage of the number of enriched genes relative to the total number of genes in the pathway.

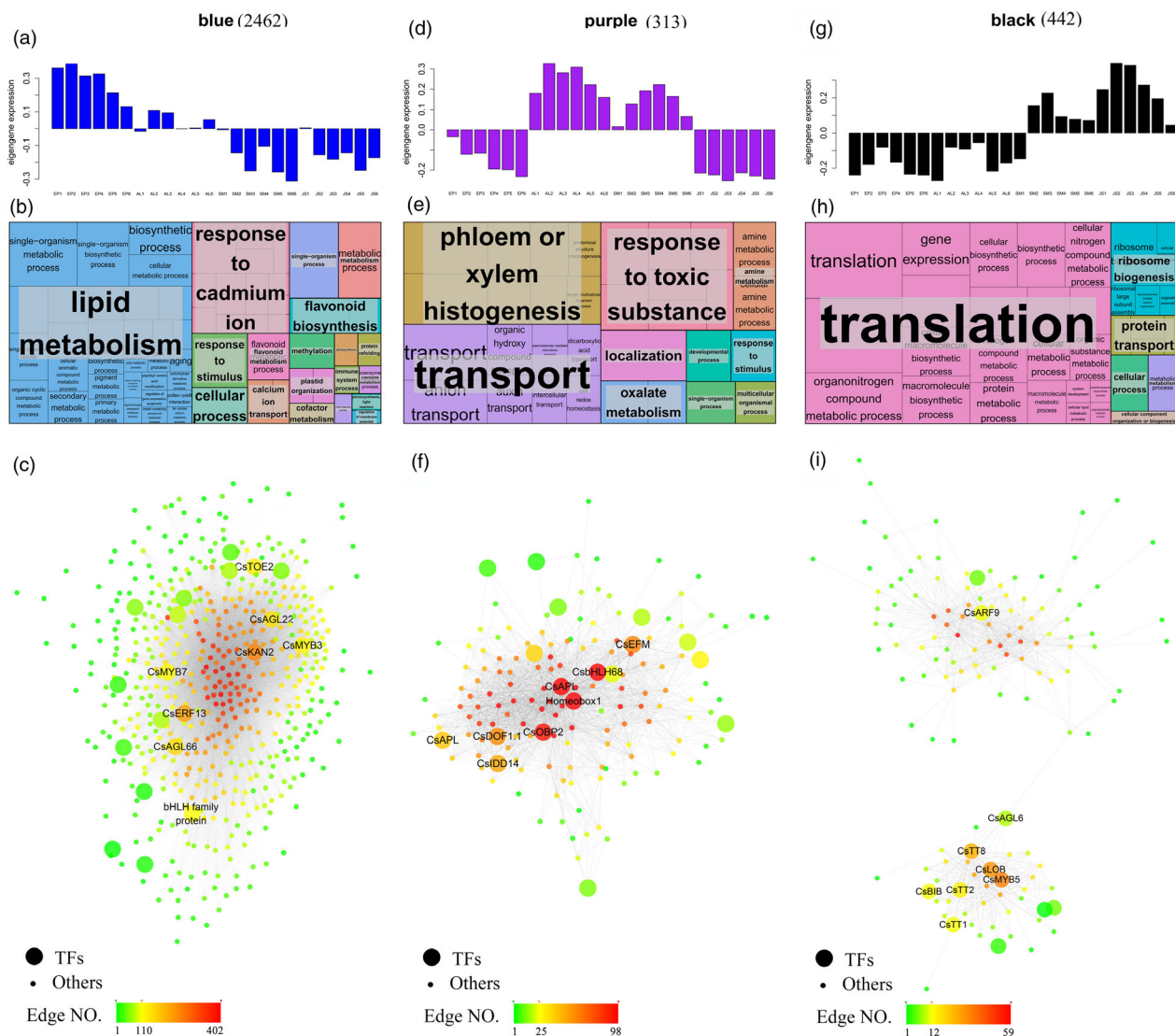


Figure 3 Expression profiles, functions and networks of tissue-specific genes. (a, d, g), Eigengene expression profiles and heat map showing the FPKM of each gene in the blue, purple and black modules. The y-axis indicates the value of the module eigengene or the gene; the x-axis indicates the sample type and developmental stage. The number of genes in each module is indicated at the top. (b, e, h) GO term enrichment analysis results of the blue, purple and black module genes visualized by the 'TreeMap' view of REVIGO. Each rectangle is a single cluster representative. The representatives are joined into 'superclusters' of loosely related terms, visualized with different colours. The size of the rectangles is adjusted to reflect the P-value. (c, f, i) Correlation networks of the blue, purple and black modules are visualized by Cytoscape. The transcription factors are shown by large circles.

substance metabolism' and 'response to stimulus' (Figure 4d, e; Table S7). Moreover, the gene networks of the green and yellow modules were also constructed and the hub genes were highlighted (Figure S3; Table S8). In addition, in the brown module, the genes were continually down-regulated or up-regulated in all four tissues across the six developmental stages and mainly involved in the 'response to chemical', 'cellulose metabolism', 'cell death' and 'cell wall organization' biological processes (Figure 4f, g; Table S7). Notably, five Expansin genes were identified in the brown module (Table S6), and they were largely up-regulated during the expansion period (Figure S4). For example, *Expansin-A1* (Cs5g10820) was up-regulated by 180-fold in the EP. Moreover, the promoter regions of three highly expressed Expansion genes (*Expansion-A8* (Cs7g29830) and

Expansion-A1 (Cs5g10820 and Cs7g03630)) contained ABA-, gibberellin (GA)- and JA-responsive elements (Table S9).

Spatiotemporal distribution of hormone-related gene expression

We identified *C. sinensis* gene families involved in the synthesis, catabolism, transport, conjugation and signalling of phytohormones (ABA, auxin, JA, GA, ETH, cytokinin, brassinosteroid and salicylic acid) by BLAST using *Arabidopsis* protein sequences as queries (Table S10). The \log_2 FPKM values for these hormone-related genes were subjected to a hierarchical clustering analysis (Figure 5b, d and f; Figure S5). In addition, the levels of ABA, IAA and JA in each fruit tissue across the six developmental stages were also determined (Figure 5a, c and e; Table S11).

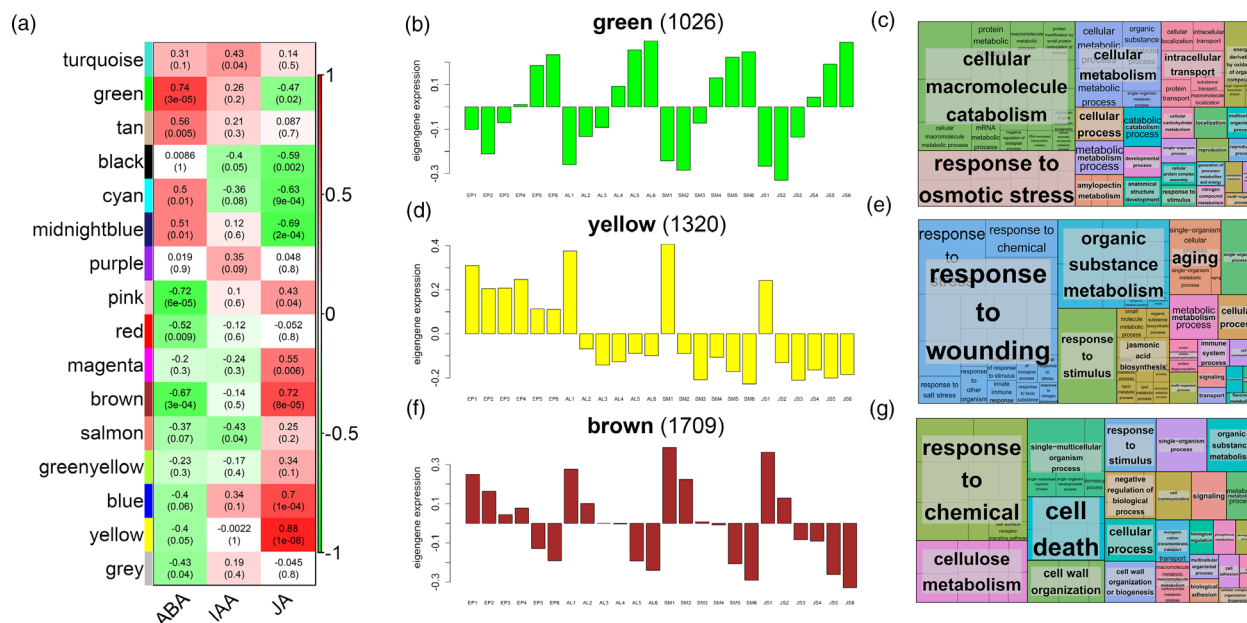


Figure 4 Expression profiles, functions and correlations of stage-specific genes. (a) Module-phytohormone association. Each row corresponds to a module. Columns correspond to ABA, IAA and JA. The colour of each cell at the row–column intersection indicates the correlation coefficient between the module and the hormone. The red-coloured cell indicates a positive correlation, and the green-coloured cell means a negative correlation. The values in each cell indicate the correlation coefficient and *p*-value. (b, d, f) Eigengene expression profiles and heat map showing the FPKM of each gene in the green, yellow and brown modules. The y-axis indicates the value of the module eigengene or the gene; the x-axis indicates the sample type and developmental stage. The number of genes in each module is indicated at the top. (c, e, g) The results of the GO term enrichment analysis of the green, yellow and brown module genes visualized by the 'TreeMap' view of REVIGO. Each rectangle is a single cluster representative. The representatives are joined into 'superclusters' of loosely related terms, visualized with different colours. The size of the rectangles is adjusted to reflect the *P*-value.

As shown in Figure 5a, the levels of ABA in the four fruit tissues increased with fruit development and the contents of ABA were different among these four fruit tissues. Notably, the ABA content in the SM was increased by approximately 3-fold at the stage of the expansion period (120–155 DAF) and remained stable during the colouring and ripening periods. The ABA level in the EP was increased by 3.95-fold to 45-fold after 120 DAF and peaked at 220 DAF. The contents of total carotenoids in the four fruit tissues across the six developmental stages were measured (Figure S5f), and no relationship was observed between the content of ABA and that of total carotenoids in the four fruit tissues. In accordance with the ABA levels, the ABA biosynthesis genes *NCED1/2/3/4*, *AAO3* and *AAO3-like* and the ABA transport genes *ABCG40* and *NRT1.2* were increasingly up-regulated in the four fruit tissues with fruit development (Figure 5b). However, ABA catabolism genes showed different expression patterns among the four fruit tissues. For example, *CYP70A1* was predominantly expressed in the EP and highly expressed during the early developmental stages in all fruit tissues (Figure 5b). Therefore, the genes involved in biosynthesis, transport, catabolism and conjugation co-regulated the content of ABA in each fruit tissue. Moreover, the expression patterns of several genes in the ABA signalling transduction model 'PYR/PYL/RCAR-PP2Cs-SnRK2s-ABFs' were in accordance with the ABA levels, including *PP2C8/51*, *SnRK2.1/2.4/2.8* and *ABF2* (Figure 5b). This finding indicates that these genes may respond to ABA during citrus fruit development. Importantly, *ABF2* (Cs3g23480) is the last gene in the ABA signalling transduction model.

The trend curves of IAA content in the four fruit tissues are shown as inverse V shapes (Figure 5c). The levels of IAA in the SM

and JS peaked at 120 DAF, while those in the EP and AL peaked at 155 DAF (Figure 5c). Auxin biosynthesis genes and efflux and influx transporters exhibited marked tissue or stage specificity (Figure 5d). The auxin biosynthesis genes *YUCCA5* and *YUCCA10* were specifically highly expressed in the EP, while *YUC3* was specifically highly expressed in the JS. These genes were up-regulated with the progression of fruit development. The auxin efflux transporters were mainly expressed in the EP, AL and SM or at 50 DAF in the four fruit tissues, with *PILS1*, *PILS6*, *PILS7* and *PIN3* highly expressed in the EP and *PIN1*, *PIN3*, *PIN5* and *PIN6* highly expressed in the AL and SM. An exception to this pattern was *PILS2*, which was highly expressed in the SM and JS at the ripening stages (Figure 5d). Auxin influx transporters such as *LAX1*, *LAX2* and *LAX3* were mainly expressed in the AL, SM and JS (Figure 5d). Taken together, these data suggest that the EP and JS may be the synthesis sites of auxin, which is then transported to other fruit tissues.

In the auxin signalling transduction pathway, the auxin receptor genes *AFB3* and *TIR1* were expressed in all fruit tissues but showed up-regulation at 155–220 DAF in the EP and AL (Figure 5d). The *AUX/IAA*, *ARF* and *SAUR* genes exhibited clear tissue or stage specificity. For instance, *AUX2* and *IAA4* were mainly expressed in the EP, and *SAUR42* was specifically expressed in the JS at the first three developmental stages (Figure 5d). GH3 proteins catalyse the conjugation of IAA to amino acids, thereby reducing free IAA (Staswick *et al.*, 2005) and forming a negative feedback loop to control auxin homeostasis. In this study, six GH3 genes were identified, namely *DFL1*, *DFL2*, two *GH3.1* genes, *GH3.6* and *GH3.9*. Among these six GH3 genes, only *GH3.1* (Cs1g22140) was dramatically up-regulated

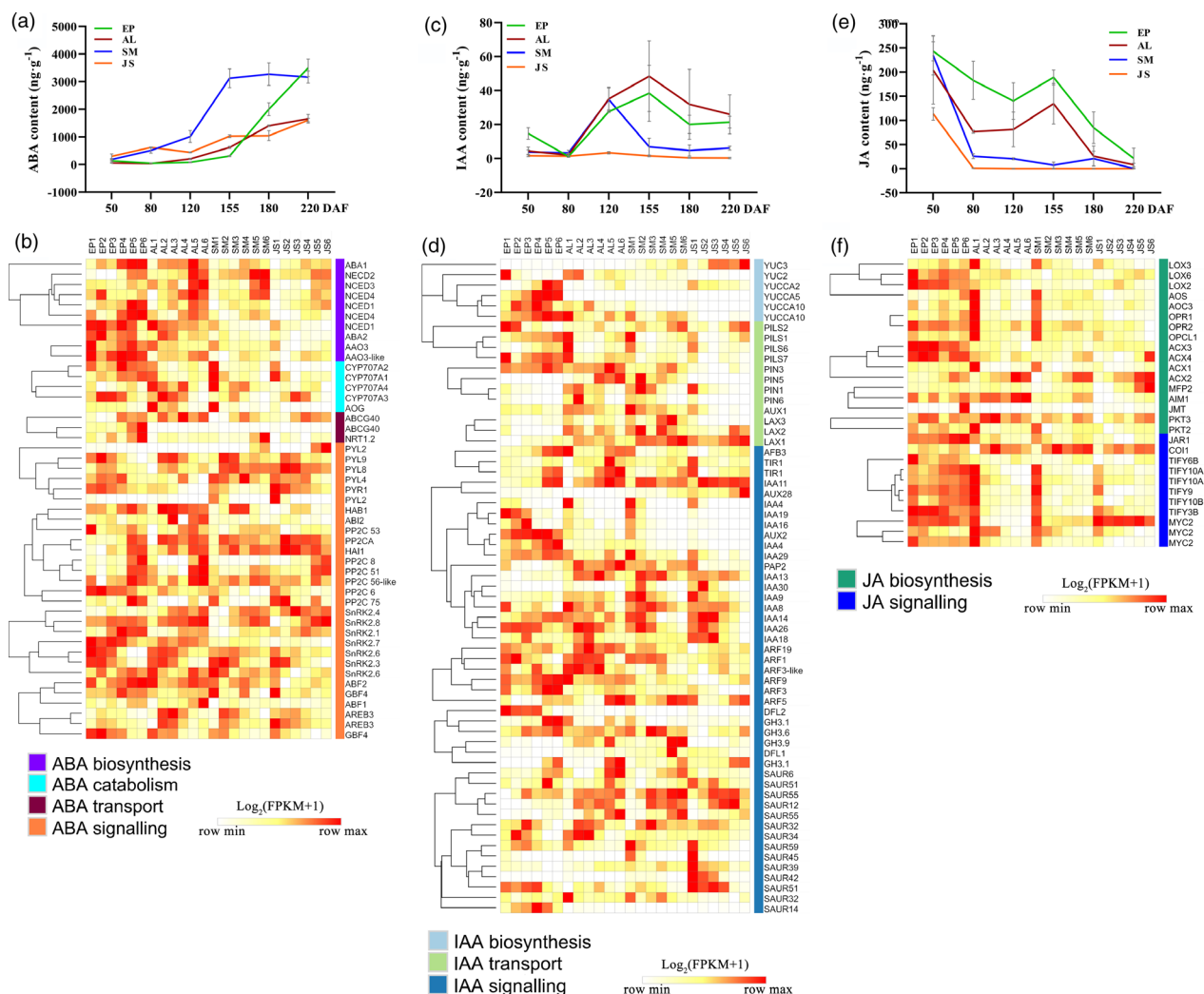


Figure 5 Dynamic changes in ABA (a), IAA (c) and JA (e) levels in the four fruit tissues during fruit development and ripening and the expression of major ABA- (b), auxin- (d) and JA-related genes (f) across tissues and stages.

(from 5.3-fold to 177-fold) after 155 DAF in all four fruit tissues, at which stage the IAA content declined by 1.46-fold to 3.75-fold in all four fruit tissues (Figure 5c, d). Hence, we hypothesized that *GH3.1* might play an important role in IAA homeostasis.

As shown in Figure 5e, our data indicate that JA was mainly contained in the EP and AL tissues except at 50 DAF and that the JA contents in the SM and JS were much lower than those in the EP and AL from 80–155 DAF. In the EP and AL, the JA levels were moderately increased at 80 or 120 DAF, peaked at 155 DAF, tapered off at 180 DAF, and reached almost zero at 220 DAF. This result was in accordance with the expression patterns of the JA synthesis and signalling genes. As shown in Figure 5f, JA synthesis and signalling genes were highly expressed in the EP at all stages and highly expressed in all fruit tissues at 50 DAF. Together, these results suggest that JA mainly plays roles in the EP and AL during citrus fruit development and ripening.

The expression profiles of the genes related to the other five phytohormones also showed significant tissue-specific or stage-specific characteristics (Figure S5; Table S10). Most of the ETH-related genes, such as ETH biosynthesis genes (*ACS1*, *ACS6*, *ACS9*, *ACO1* and *ACO4*) and signalling genes (*ERF1* and

ERF2), were highly expressed in fruit at the early developmental stage (50–80 DAF); moreover, several genes were highly expressed in the EP and AL, including *ACO2*, *ACO4*, *EIN3* and *EBF1/2* (Figure S5a). Most of the GA-related genes gradually decreased after 120 or 155 DAF, while the expression of the *GID1s* and *PIF3* genes dramatically increased from 155 or 180 DAF (Figure S5b). The expression of salicylic acid-related genes gradually increased in all fruit tissues with development (Figure S5c). There were not clear patterns in the cytokinin and brassinosteroid genes, which indicated the complicated regulatory networks of these two phytohormones during citrus fruit development. (Figure S5d, e).

Excavation of key genes involved in sugar and acid accumulation of *C. sinensis* fruit

The taste of citrus fruit is determined by the content of soluble sugars and organic acids. In ripe citrus fruit, sucrose, fructose and glucose are the main soluble sugars, and citric acid and malic acid are the main organic acids. In this study, the soluble sugars in the fruit pulp rapidly accumulated from 80 DAF and moderately accumulated from 155 DAF (Figure 6a). For organic acids, the content of citric acid in the fruit pulp increased dramatically at the

early developmental stages, peaked at 80 DAF and tapered off from 80–220 DAF, whereas the content of malic acid peaked at 80 DAF, declined at 120 DAF, and moderately increased from 155 DAF. The content of quinic acid was constantly decreased and reached almost zero at 220 DAF (Figure 7a).

Citrus fruit primarily directly accumulates sucrose. Hence, the regulation of source-to-sink sucrose transport is vital for sugar accumulation in citrus fruit JSs. In this study, we identified 13 *SWEET*, 3 *SUT* and 2 *TMT* sucrose transporters (Table S10). As shown in Figure 6b, these sucrose transporters were differentially spatiotemporally expressed in *C. sinensis* fruit during the six developmental stages. For example, *SUT4*, *TMT1*, *TMT2* and *SWEET16* were expressed in all four fruit tissues and their expression levels increased with fruit development. Interestingly, we noted that *SWEET15* was specifically highly expressed in the SM and JS, and *SWEET10* was specifically highly expressed in the SM. Moreover, the expression levels of *SWEET10* and *SWEET15* were increasingly up-regulated with fruit development (Figure 6b). A phylogeny analysis showed that *SWEET10*, *SWEET12* and *SWEET15* were clustered together (Figure S6b), which

indicated that these genes have similar functions. Moreover, the expression level of *SWEET15* was positively correlated ($R^2 = 0.8763$) with the content of fruit sugar in 'Anliu' orange and its high sugar bud sport 'Honganliu' orange (Figure 6c; Figure S6d). This relationship and the tissue-specific expression pattern were further verified in different citrus varieties, including sweet oranges ($R^2 = 0.7758$), loose-skin mandarins ($R^2 = 0.8254$) and pummels/grapefruits ($R^2 = 0.7293$; Figure S6c, d and e). Furthermore, a fluorescence *in situ* hybridization assay was used to characterize the expression pattern of *SWEET15* in the JS. As shown in Figure 6d, *SWEET15* was expressed in the epidermal cells of the JS. In addition, the genes involved in sucrose biosynthesis and catabolism were also identified (Table S10), and the expression patterns of most of these genes in the four fruit tissues were similar except *CWINV5* and *SBPase* (Figure S6a). Most of the sucrose biosynthesis genes, such as *SPS1/2*, *SPP1* and *CCR4A*, were up-regulated during the ripening stages in the four fruit tissues, while most of the sucrose synthase genes, such as *SUS1/3*, hydrolysed sucrose either to fructose and UDP-glucose, were increasingly down-regulated with fruit development

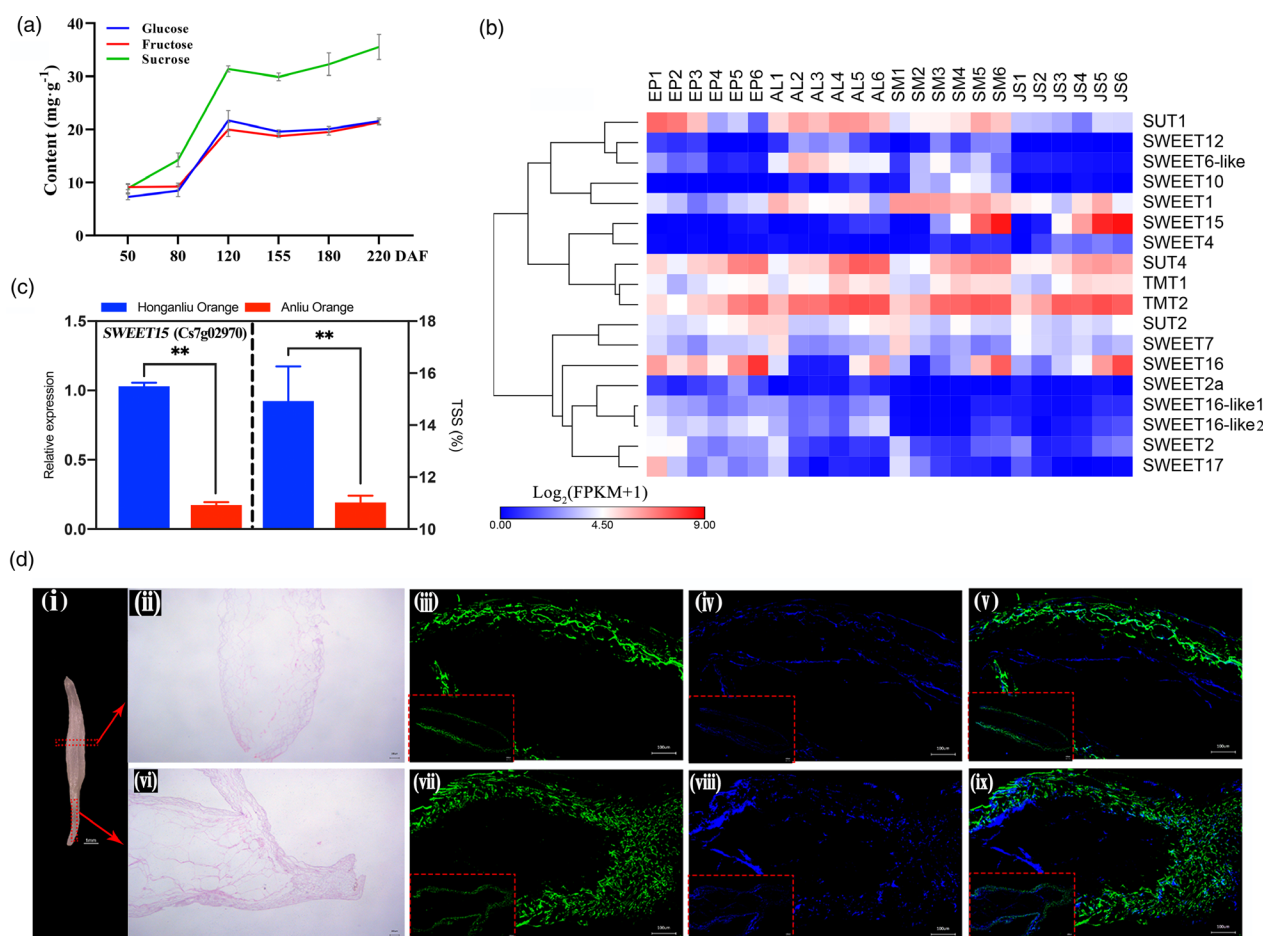


Figure 6 Expression of genes related to sugar accumulation in citrus fruit across tissues and stages. (a) Soluble sugar content in the pulp at each stage. (b) Expression of sucrose transport-related genes across tissues and stages. (c) Expression of *SWEET15* and content of total soluble solids (TSSs) in 'Anliu' orange and its bud sport 'Honganliu' orange. (d) *In situ* hybridization analysis of *SWEET15* in the juice sac at fruit ripening stage. The juice sac (i) was sampled at 150 DAF. *SWEET15* expression is detected with green fluorescent probes in the epidermal layers of the juice sac in the transverse section (ii) and vertical section (vi). (iii–v, vii–ix) Whole images of the transverse section and vertical section of the juice sac are indicated by a red frame at the left bottom. (ii, vi) Paraffin sections. Blue colouration represents nuclei stained by DAPI (iv, viii). The *SWEET15* expression and nuclear images are merged (v, ix). (i) Scale bar = 1 mm. (ii–ix) Scale bar = 100 μ m. Double asterisks represent statistically significant differences ($P < 0.01$) analysed using Student's *t*-test. DAF: days after flowering.

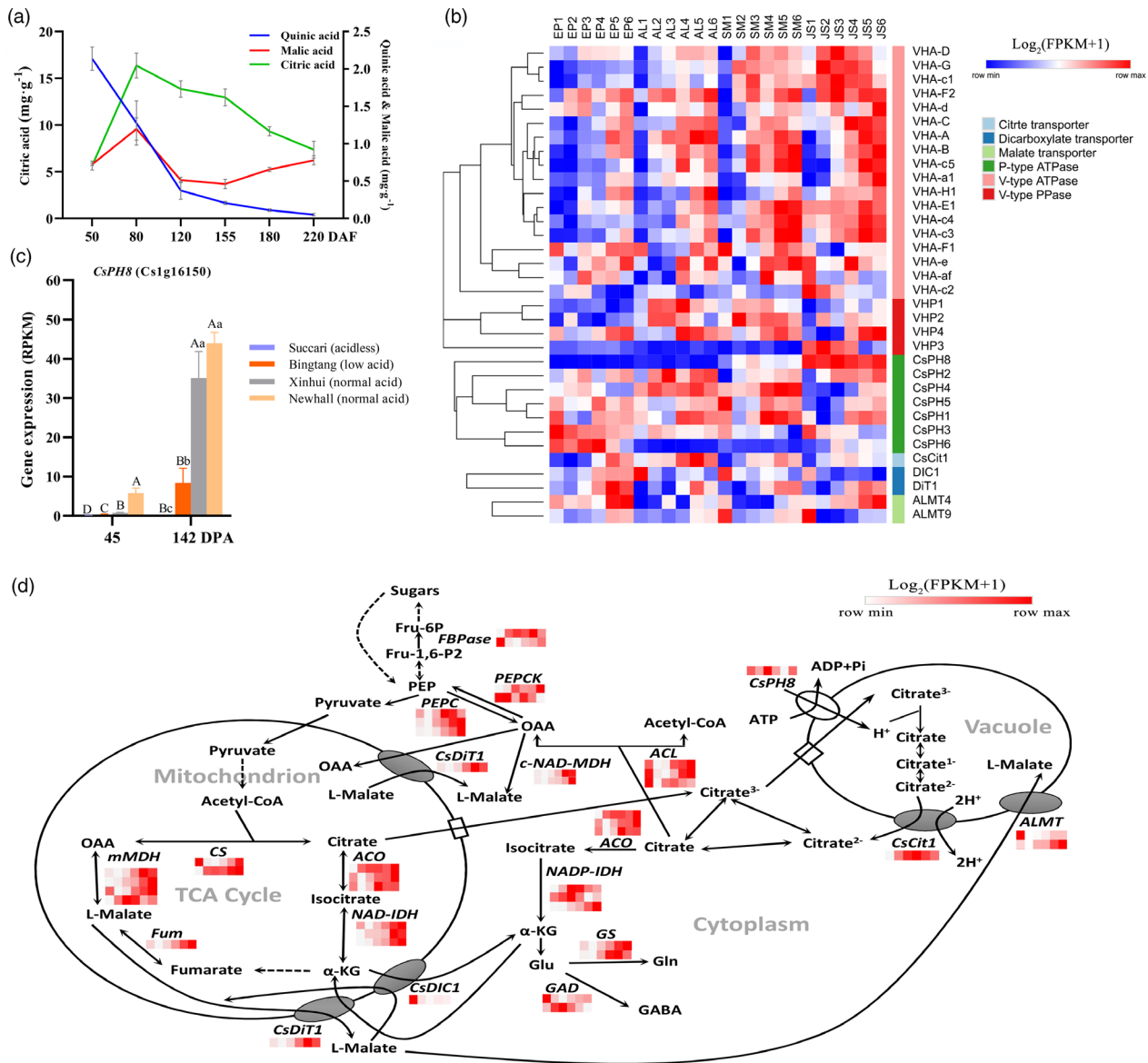


Figure 7 Expression of genes related to acid accumulation in citrus fruit across tissues and stages. (a) Content of organic acids in pulps at each stage. (b) Expression of citric acid and malic acid transport-related genes across tissues and stages. (c) Expression patterns of *CsPH8* in four different orange varieties. (d) Temporal expression patterns of the genes involved in citric acid and malic acid metabolism in juice sac cells during citrus fruit development and ripening. ACO: aconitase, ACL: ATP-citrate lyase, ALMT: aluminium-activated malate transporter, α -KG: α -ketoglutarate, CS: citrate synthase, NAD-IDH: NAD-dependent isocitrate dehydrogenase, NADP-IDH: NADP-isocitrate dehydrogenase, Fum: fumarase, c-NAD-MDH: NAD-dependent malate dehydrogenase, mMDH: mitochondrial malate dehydrogenase, FBPase: Fructose-1,6-bisphosphatase, Glu: glutamate, Gln: glutamine, GS: glutamine synthetase, GAD: glutamate decarboxylase, GABA: γ -aminobutyric acid, OAA: oxaloacetate, PEPC: Phosphoenolpyruvate carboxylase, PEPCK: phosphoenolpyruvate carboxykinase. DAF: days after flowering. DPA: days post-anthesis.

(Figure S6a). However, several invertase genes (which hydrolysed sucrose to glucose and fructose) displayed different expression patterns. Vacuolar invertase (*bFrut1*) and cell wall invertase (*INV4*) were increasingly up-regulated with fruit development in the four fruit tissues, while cell wall invertase *INV3* was the opposite (Figure S6a).

Citric acid is the main organic acid in citrus fruit. Hence, we identified the genes in the four fruit tissues that were involved in citric acid biosynthesis, catabolism and transport (Table S10). Previous studies showed that the influx and efflux of organic acid from vacuoles and mitochondria were important for organic acid accumulation in citrus fruit (Aprile *et al.*, 2011; Hussain *et al.*,

2017; Shi *et al.*, 2015; Shimada *et al.*, 2006). Therefore, we specifically excavated the genes related to citrate and malate transport (Figure 7b; Table S10). As shown in Figure 7b, most of the H⁺ ATPase genes were increasingly up-regulated with fruit development in all fruit tissues. In particular, *CsPH8* (*AHA10*) was specifically expressed in the SM and JS and highly expressed in the JS. Then, we analysed the expression of *CsPH8* in four different citrus varieties ('Succari', 'Bingtang', 'Xinhui' and 'Newhall'); the citric acid contents of these varieties were highly variable. We observed that the expression of *CsPH8* was highly correlated with the content of citric acid (Figure 7c). Further, three TFs, *MYB5* (Cs9g03070), *TT8* (Cs5g31400) and *CPC* (Cs2g21750), were

highly coexpressed with *CsPH8* (Figure S7b, c). In addition, *CsCit1*, which mediates citrate efflux from vacuoles, and *ALMT4* and *ALMT9*, which mediate malate influx into vacuoles, were up-regulated in all fruit tissues. These findings were consistent with the content of citric acid and malic acid. Moreover, the genes involved in citric acid biosynthesis and catabolism also regulated the accumulation of citric acid. Most of the genes involved in citric acid biosynthesis and catabolism showed the same expression patterns in the four fruit tissues, and their expression was continuously up-regulated with fruit development (Figure S7a). To further identify the key genes involved in the regulation of citric acid and malic acid metabolism, we constructed a gene expression regulation network diagram for the JS tissue (Figure 7d).

Exogenous ABA analogue promoted citrus fruit ripening

According to the results of the transcriptome analysis, ABA plays significant roles in different biological processes during different stages of citrus fruit development. Therefore, we tested the effect of the application of the exogenous ABA analogue AM1 on citrus fruit development in Satsuma mandarin. AM1 significantly promoted citrus fruit colouring, chlorophyll degradation and sugar accumulation (Figure 8a-d), and decreased the content of IAA in both the fruit peel and pulp (Figure 8e); the AM1-mediated promotion of sucrose accumulation was especially notable (Figure S8). Further, we used qRT-PCR to quantify many genes in different pathways, including the IAA conjugation (Figure 8f), cell wall metabolism (Figure 8g), carotenoid biosynthesis, ABA signalling (Figure 8h), chlorophyll degradation (Figure 8i) and sugar transport pathways (Figure 8j). Notably, the expression of several genes, such as *ABF2*, *RRCR*, *SWEET15* and *GH3.1*, was largely up-regulated by AM1 (Figure 8). These results revealed that ABA is crucial for citrus fruit development and ripening.

ABF2 plays a master role in ABA signalling during *C. sinensis* fruit ripening

According to the results above, *ABF2* is the key gene that mediates ABA signalling. We identified several genes that were coexpressed with *ABF2* and contained at least one ABA-responder *cis*-element (CACGTG or ACGTG) in the promoter (Figure 9a). These genes included carotenoid and ABA biosynthesis genes (*PSY*, *Z-ISO*, *NCED1/2/4*), chlorophyll catabolism genes (*HCAR*, *PAO*, *RCCR*, *PPH* and *NYC1*) (CCEs), sugar transporter genes (*SUT4*, *SWEET10/15/16*), an IAA conjugation gene (*GH3.1*) and fruit enlargement- and softening-related genes (*Expansin-A1/A8*). The interaction between *ABF2* and several of these genes was further verified by yeast one-hybrid (Y1H) assays or dual-luciferase assays (Figure 9b, c). According to the transcriptome data and verification assays, a model was proposed to illustrate the ABA signalling regulation network mediated by *ABF2* in citrus fruit (Figure 10a). In this model, *ABF2* plays a master role and is involved in the regulation of sucrose transport, chlorophyll degradation, auxin homeostasis, carotenoid and ABA biosynthesis, and fruit enlargement and softening.

Discussion

Citrus fruits are classified as hesperidium fruits with a unique structure. Using manual dissection, four different types of *C. sinensis* fruit tissues were isolated across the whole fruit

development and ripening period, and RNA-seq was performed. The comprehensive two-dimensional tissue and stage collection and in-depth RNA-seq data set enable genome-scale analyses at a high resolution.

Difference among the transcriptomes of the four fruit tissues

In this study, many tissue-specific genes were identified in each fruit tissue, which may contribute to the difference among the four fruit tissues. For instance, several coexpressed gene sets were identified by the WGCNA, such as the blue, purple and black modules (Figure 3a, d and g). These tissue-specific gene sets were enriched in different biological processes (Figure 3b, e and h). Notably, the expression of the genes involved in ABA, IAA and JA biosynthesis showed significant tissue specificity, which resulted in differences in the dynamic changes in ABA, IAA and JA content among the EP, AL, SM and JS (Figure 5). In addition, several key sucrose and citric acid accumulation genes, such as *SWEET15* and *CsPH8*, also showed tissue-specific expression patterns (Figures 6b, 7b). Previous studies in strawberry (Hollender *et al.*, 2014; Kang *et al.*, 2013), maize (Zhan *et al.*, 2015), tomato (Pattison *et al.*, 2015) and *Populus tremula* (Sundell *et al.*, 2017) indicated that tissue-specific transcriptome analyses could reveal a more refined regulation network or novel regulatory mechanisms. Hence, these studies emphasize the importance of tissue-based omics approaches and highlight the potential pitfalls that are inherent in whole fruit or mixed tissues omics research.

Insights into the ABA regulatory network during citrus fruit development and ripening

ABA plays a crucial role in fruit development and ripening. Previous studies indicate that ABA treatment can increase the sugar content in apple (Ma *et al.*, 2017) and citrus fruit (Kojima *et al.*, 1995; Wang *et al.*, 2016), regulate anthocyanin accumulation in grape (Berli *et al.*, 2011), alter the production of carotenoids in tomato (Kachanovsky *et al.*, 2012; Sun *et al.*, 2012b), and also modify the expression of fruit softening-related genes (Sun *et al.*, 2012a), such as Expansin (Brummell *et al.*, 1999). In this study, the AM1 treatment showed that ABA regulates various metabolic pathways related to citrus fruit ripening, including sugar accumulation, chlorophyll degradation, carotenoid and ABA biosynthesis, cell wall metabolism and IAA homeostasis (Figure 8). Several studies revealed that ABA played important roles and might interact with different regulators (such as ethylene, jasmonic acid and sucrose) during citrus fruit ripening (Alferez and Zacarias, 1999; Goldschmidt, 1998; Wu *et al.*, 2014b; Zhang *et al.*, 2015). In addition, ABA was reported to participate in regulating the colour of citrus fruit peel and might be a feedback regulator of carotenoid metabolism (Rodrigo *et al.*, 2003; Zhu *et al.*, 2017). However, the mechanism and networks of the ABA-mediated regulation of multiple metabolic pathways during citrus fruit development and ripening remain unresolved. In this study, we identified an *ABF2* (Cs3g23480) gene, and its expression was positively correlated with the level of ABA. Our data showed that *ABF2* could positively respond to ABA and regulate multiple genes distributed in multiple metabolic pathways (Figures 8 and 10a). Interestingly, in this study, we found that when the ABA contents rapidly increased or reached a certain concentration, a decrease in the IAA levels was accompanied in all four fruit tissues (Figure 5a, c). This phenomenon was also observed in strawberry fruit

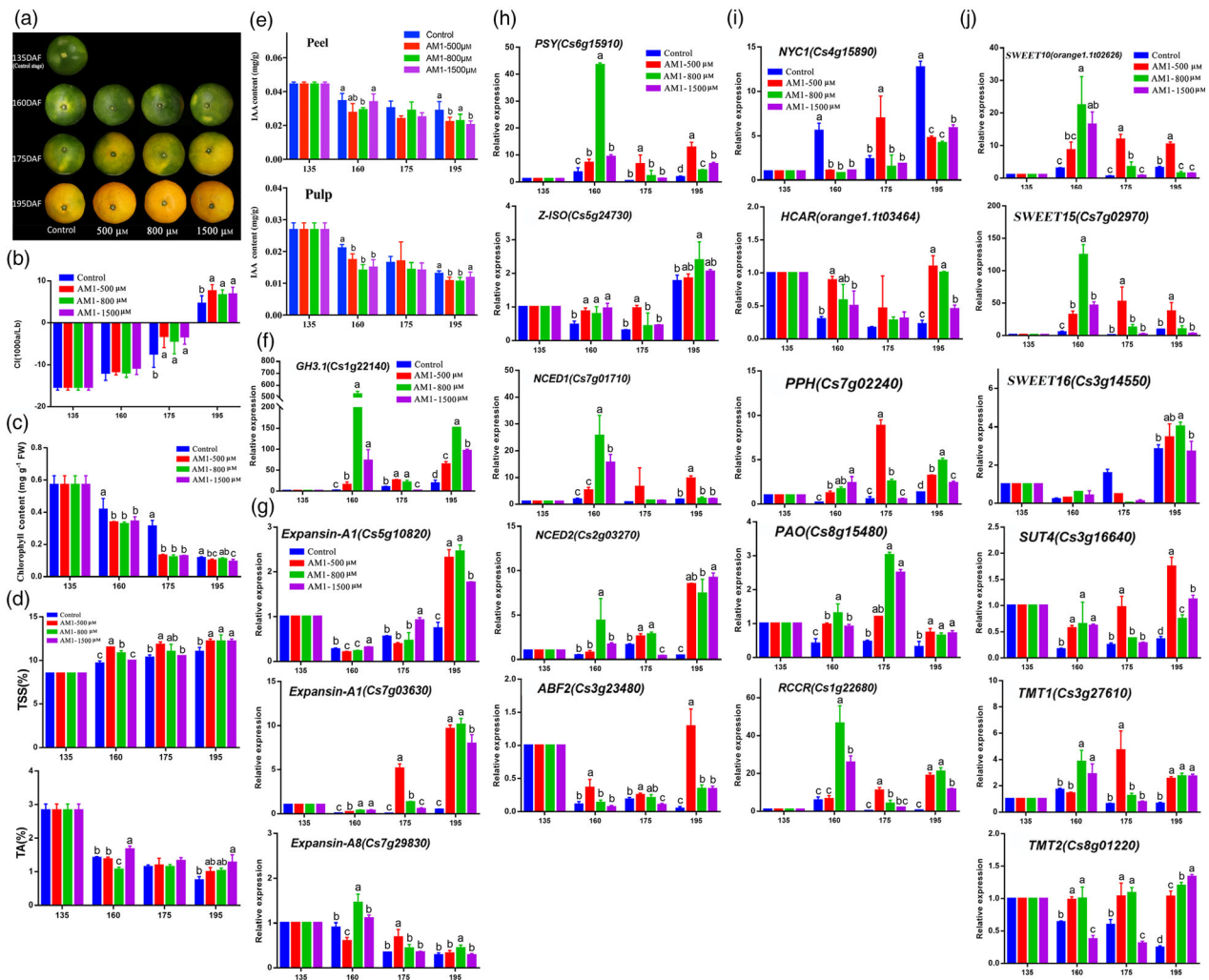


Figure 8 Citrus fruit development and ripening promoted by ABA analogue. (a) Fruits sampled at different developmental stages from the trees treated with three different concentrations of AM1. (b) Colour index (CI) of the fruit peel. (c) Chlorophyll content of the fruit peel. (d) Total soluble solid (TSS) and total titratable acid (TA) contents in the fruit pulp. (e) IAA content in the fruit peel and pulp. (f) Relative expression of the genes related to IAA homeostasis (f), cell wall metabolism (g), carotenoid and ABA biosynthesis (h), chlorophyll degradation (i) and sugar transport (j). Lowercase letters represent statistically significant differences ($P < 0.05$) analysed using a one-way ANOVA. DAF: days after flowering.

(Archbold and Dennis Jr, 1984). Moreover, the AM1 treatment could decrease the contents of IAA in both the citrus fruit peel and pulp (Figure 8e). Indeed, we also observed that the auxin conjugation gene *GH3.1* was highly expressed, which was promoted by *ABF2* (Figure 9c), and accompanied by a decrease in IAA levels (Figure 5c, d). Hence, we propose that ABA is involved in regulating auxin homeostasis through *ABF2* and *GH3.1*. In addition, we found that ABA could promote the expression of the key ABA biosynthesis genes *NCEDs* and key carotenoid metabolism gene *PSY* (Figure 8h), the promoters of which could interact with *ABF2* (Figure 9). These results indicate that an auto-induction of ABA production (inducing its own production) pathway like ETH production (Paul *et al.*, 2012) is involved in citrus fruit ripening and represents a feedback regulator of carotenoid metabolism. Based on our data, we propose that *ABF2* is the magnifier of ABA signalling and plays diverse roles in different metabolism processes during citrus fruit development and ripening (Figure 10a).

Identification of key genes involved in sucrose accumulation in citrus fruit

Sink strength is important for photoassimilate source-to-sink translocation. Sucrose invertases and synthases (SUSYs) are important for sink strength, which is partly controlled within sink cells and/or translocation points (Sadka *et al.*, 2019). Up-regulating SUSY in cucumber induced sucrose and starch accumulation and increased fruit size (Fan *et al.*, 2019). Down-regulating acid invertase in muskmelon reduced the fruit size and sucrose level (Yu *et al.*, 2008). Similarly, the phenotypes associated with reduced sink strength were also observed in tomato and carrot by down-regulating vacuolar and cell wall invertases as well as SUSYs (D'Aoust *et al.*, 1999; Tang *et al.*, 1999). In this study, several SUSYs (*SUS1/3*), vacuolar invertase (*bFruct1*) and cell wall invertases (*INV3/4*) were highly expressed in the four fruit tissues, and the expression patterns of these genes were changed with fruit development (Figure S6a). This result indicates that

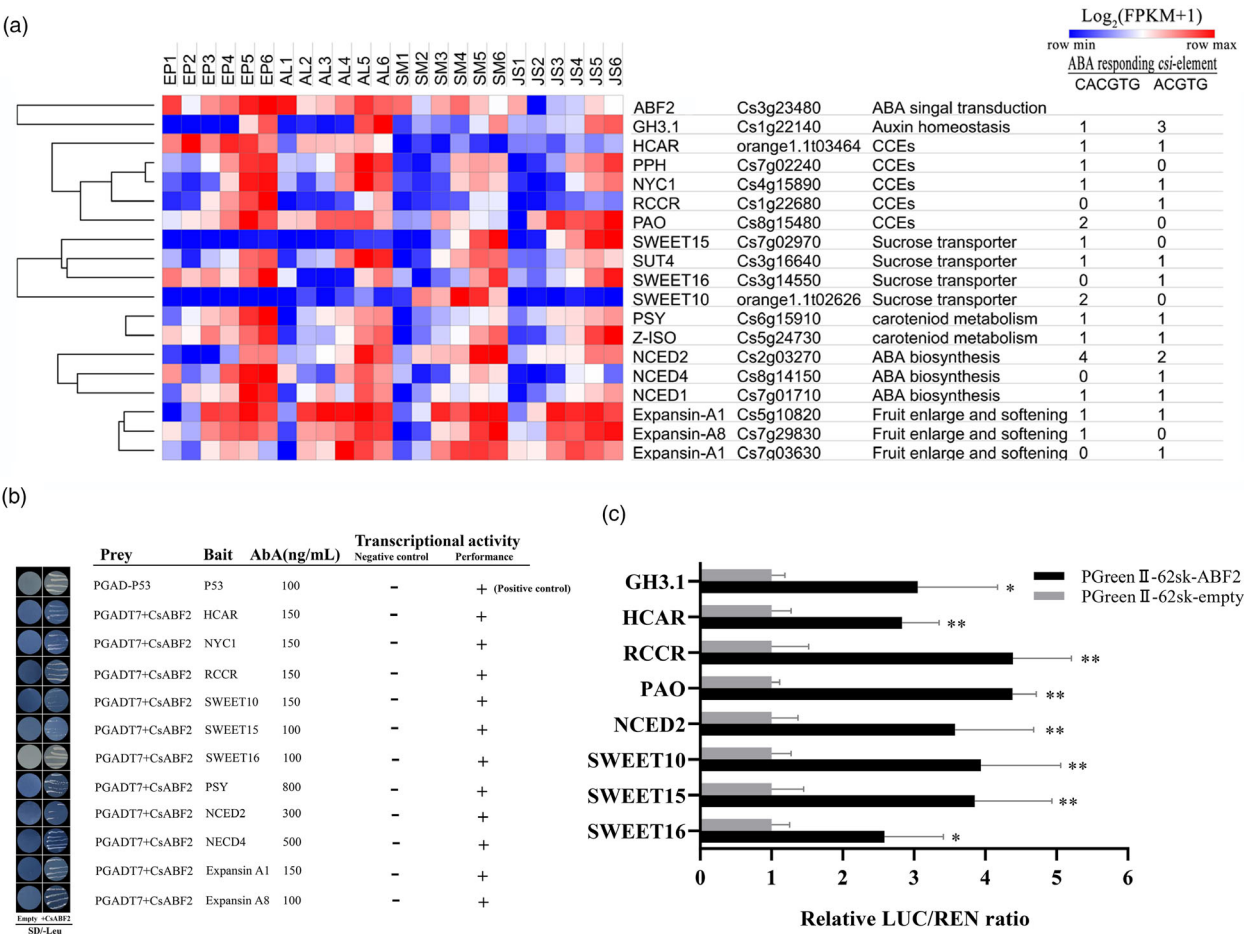


Figure 9 Genes that interacted with *ABF2*. (a) Expression patterns of the genes containing ABA-responsive (ABRE) *cis*-elements in their promoter regions. (b) Yeast one-hybrid assays verified the interactions of *ABF2* and the promoters of selected genes. The empty vector pGADT7 was used as a negative control, and p53-pABAI/pGAD-p53 was used as a positive control. Yeast cells were grown in a SD/-Leu selection medium containing the corresponding concentration of aureobasidin A (AbA). All suspensions of yeast cells in this assay were adjusted to the original concentration (OD600 = 0.1). (c) Dual-luciferase assays verified the interactions of *ABF2* and the promoters of selected genes *in vivo*. The empty pGreenII-62-SK-LUC vector was used as a negative control. Error bars represent \pm SE ($n = 4$). Asterisks indicate statistically significant differences determined by Student's *t*-test (* $P < 0.05$, ** $P < 0.01$).

these SUSYs and invertases may play roles in controlling sink strength. Phloem unloading is the key translocation point for sugar accumulation in sink tissue, which is regulated by symplasmic and apoplasmic pathways (Sadka *et al.*, 2019). In the apoplasmic pathway, the transmembrane transport of sucrose is catalysed by various sugar transporters (Aoki *et al.*, 2003). TMTs are proton-coupled antiporters capable of loading a large amount of glucose, fructose and sucrose into the vacuole, and they are localized on the tonoplast (Aluri and Buttner, 2007; Schulz *et al.*, 2011). SUTs (synonym SUCs) are another type of sucrose transporter that is classified into four distinct groups (Payyavula *et al.*, 2011). SUT4 (Group IV) is well separated from the three other groups. The SUT4 proteins from monocots and dicots were reported to be localized on either the tonoplast or plasma membranes and acted as sucroseH⁺ symporters to uptake extracellular sucrose and release sucrose from the vacuole (Schneider *et al.*, 2012; Schulz *et al.*, 2011). Islam *et al.* (2015) reported that *SUTs* might play important roles in the transport of sucrose into the citrus fruit JS. Together, TMTs and SUTs modulate soluble sugar accumulation in the vacuole (Reuscher *et al.*, 2014). In this study, we identified two *TMTs* and three *SUTs* (Figure 6b). The expression patterns of

TMT1/2 and *SUT4* were correlated with the level of sucrose, and they were expressed in all four fruit tissues (Figure 6b). However, sucrose only accumulates in the JS tissue in citrus. Hence, the *TMT* and *SUT* sucrose transporters are not the key genes. Then, we identified 13 *SWEET* sucrose transporters (Figure 6b). Notably, *SWEET10* and *SWEET15* were specifically expressed in the JS and/or SM (Figure 6b). The *SWEET* sugar transporters are divided into four clades (Chen *et al.*, 2012; Xu *et al.*, 2014). Clade III *SWEETs* appear to transport sucrose in an H⁺-independent manner and are typically involved in cellular efflux processes (Chen *et al.*, 2012; Lin *et al.*, 2014). Two clade III *SWEETs*, *SWEET11* and *SWEET12*, are localized to the plasma membrane of phloem parenchyma cells and export sucrose from these cells into the phloem apoplasm in preparation for phloem loading (Chen *et al.*, 2012). In addition, *SWEET11*, *SWEET12* and *SWEET15* mediated sucrose efflux in the transfer of sugars from the seed coat to the embryo (Chen *et al.*, 2015). In our study, *SWEET10*, *SWEET12* and *SWEET15* were clade III *SWEETs* (Figure S6b). Based on the results of the *in situ* hybridization and tissue-specific expression assays, we propose a functional model for sucrose translocation from vascular tissue to JS cells (Figure 10b). In this model, *SWEET15* plays a crucial role in the sucrose accumulation of citrus

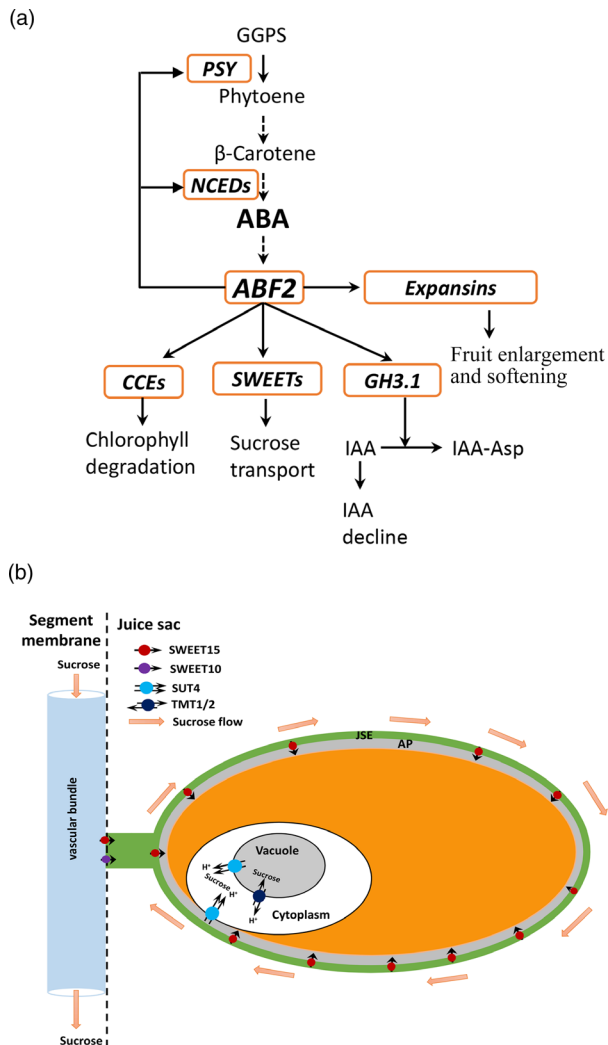


Figure 10 Models proposed for ABA signalling and sucrose accumulation. (a) ABA signalling regulation network during citrus fruit development and ripening mediated by *ABF2*. CCEs, chlorophyll catabolic enzymes. (b) Model for the multistep transport of sucrose accumulated in the juice sac initiated by SWEET, SUT and TMT sucrose transporters. JSE, juice sac epidermis; AP, apoplast.

fruit and appears to mediate sucrose release into the apoplast. Recently, a study showed that *PuSWEET15* is expressed at higher levels in BNG fruit, which is a high sugar content bud sport of Nanguo (NG) pear (*Pyrus ussuriensis*); *PuSWEET15* overexpression in NG pear fruit increased the sucrose content; and silencing of *PuSWEET15* in BNG fruit decreased the sucrose content (Li *et al.*, 2020). Nonetheless, these results were obtained based on gene expression data alone; thus, further gene function research is needed.

Symplasmic and apoplastic pathways are both observed in citrus fruit, and symplasmic pathway is suggested to be dominant (Koch *et al.*, 1986; Nli and Coombe, 1988; Sadka *et al.*, 2019). In this study, vacuolar invertase (*bFruct1*) and cell wall invertases (*INV3/4*) were expressed in the four fruit tissues (Figure S6a), which indicates that the apoplastic pathway plays a role in the four fruit tissues in sucrose translocation. Moreover, several key genes (*SWEETs*, *SUTs* and *TMTs*) were identified in the apoplastic pathway, and they may represent the key genes responsible for the accumulation of sugar in the JS. Hence, the relationship

between symplasmic and apoplastic pathways in citrus fruit should be further researched.

Identification of key genes involved in citrate accumulation in citrus fruit

The comprehensive regulation of citrate synthesis, transmembrane transport and degradation/utilization determines citrate accumulation (Cercos *et al.*, 2006b; Sadka *et al.*, 2000). In this study, we found that the expression levels of almost all genes involved in citrate metabolism were continuously up-regulated from 80 DAF (Figure 7d; Figure S7a). This result suggests that the decrease in citrate content during the late stages of fruit development was due to the up-regulation of citrate degradation or utilization pathways, including the Aco-GABA pathway (Cercos *et al.*, 2006b) and ACL pathway (Hu *et al.*, 2015). Several studies have demonstrated the important roles of ACOs in citrate accumulation (Degu *et al.*, 2011; Li *et al.*, 2017; Shlizerman *et al.*, 2007). Transient overexpression of *CitAco3* significantly reduced the citric acid content of citrus leaves and fruits (Li *et al.*, 2017). The studies on different citrus cultivars show that GAD (Liu *et al.*, 2014) and ACL (Hu *et al.*, 2015) are also involved in citrate accumulation. Moreover, a report has suggested that the low citrate of Satsuma mandarin is attributed to citrate degradation (catalysed by *CitAco3–CitGS2–CitGDU1*) and transport (mediated by *CitCHX* and *CitDIC*) (Lin *et al.*, 2015a). GABA pathway is reported to contribute to the significant citrate decrease in citrus fruit, which is associated with the expressions of ACO, GS, GAD and IDH (Lin *et al.*, 2015b; Sheng *et al.*, 2017). In this study, the spatial-temporal expression pattern of the genes involved in citrate metabolism showed significant changes during citrus fruit development, including ACLs, ACOs, NAD-IDHs, GSs, GADs, *CsDIC1* and *CsDIT1* (Figure 7d). This result suggests that each gene in this network might influence citrate accumulation.

The acidity of citrus fruit is dependent on citrate accumulation in the JS cell vacuole. When citrate is transported to the cytoplasm, the uptake of citrate into the vacuole depends on the activity of the proton pumps (Brune *et al.*, 2002; Muller *et al.*, 1996). Here, we found that the p-type proton pump gene *CsPH8* (synonym *AHA10*) was specifically highly expressed in the JS tissue (Figure 7b). Further, we analysed the expression of citrate metabolism-related genes in four different citrus varieties, the acidity of which ranged from non-acidic to normal acidity. The *CsPH8* gene was differentially expressed among the four varieties of fruit, and its expression was positively related to acidity (Figure 7c). Aprile *et al.* (2011) found that the *AHA10* gene was not expressed in no-acid lemon but highly expressed in the wild-type sour lemon. Shi *et al.* (2015) also found that the expression of *CsPH8* in the 'Honganliu' orange (low acid) was lower than that in the 'Anliu' orange (normal acid), and overexpression of *CsPH8* in acidless pumelo JSs, strawberry fruit, and tomato fruit significantly increased the titratable acid or citric acid content (Shi *et al.*, 2019). Moreover, Strazzer *et al.* (2019) reported that the expression of *CitPH1* and *CitPH5* (*AHA10*) was strongly reduced in acidless citrus varieties, and down-regulation of *CitPH1* and *CitPH5* was associated with mutations that disrupt the expression of MYB, HLH and/or WRKY transcription factors. In this study, three TFs, *MYB5* (Cs9g03070), *TT8* (Cs5g31400) and *CPC* (Cs2g21750), were highly coexpressed with *CsPH8* (Figure S6e, f). Hence, these genes may be involved in regulating the expression of *CsPH8* and could play important roles in citrate accumulation. Taken together, we propose that *CsPH8* and its regulation genes may play significant roles in citrate transport or

storage in vacuoles of citrus JS cells and could have a dramatic influence on citrate accumulation.

Conclusion

In summary, the high spatial and temporal resolution of transcriptome data provides significant insights into citrus fruit development and ripening, including the identification of several tissue-specific modules and hub TFs, the discovery of the ABA signalling regulatory network during citrus fruit development and ripening, the interaction between ABA and auxin signalling, and the identification of key genes involved in sucrose accumulation and citrate metabolism.

Materials and methods

Plant materials, sample collection and tissue isolation

Fruit samples of the 'Fengjie 72-1' navel orange (*C. sinensis* L. Osbeck) were harvested at 50, 80, 120, 150, 180 and 220 DAF. Three trees were used as one biological replicate. Three biological replicates (three trees per replicate) were harvested at each developmental stage. Twelve representative fruits were sampled from each tree at each developmental stage. After isolating the four fruit tissues (EP, AL, SM and JS) by manual dissection, the samples were rapidly frozen in liquid nitrogen and stored at -80°C . A portion of the samples was used for extracting the total RNA, as described previously (Liu *et al.*, 2006), and the other portion of the sample was used for the determination of phytohormones, soluble sugar and organic acid.

RNA-seq and data processing

Twenty-four samples of the four fruit tissues across six developmental stages were harvested, and three biological replicates were harvested for each sample. A total of 72 transcriptome profiles were obtained by RNA-seq using the Illumina HiSeq™ 4000 sequencing platform at Novogene (Beijing, China). The sequencing raw data have been submitted to the NCBI Gene Expression Omnibus (GEO) under the accession number GSE125726. The raw transcriptomic data of 24 pulp samples from four varieties of sweet orange (*C. sinensis* L. Osbeck) (Newhall, Xinhui, Bingtang and Succari) were downloaded from the NCBI Sequence Read Archive (SRA) (accession number: SRP070469) (Huang *et al.*, 2016). The samples of these four varieties fruits were collected at 45 and 142 days post-anthesis (DPA). The method for data processing is detailed in our previous publication (Feng *et al.*, 2019).

Expression data analysis

The expression modules in Figure 2a were generated by STEM v1.3.7 (Ernst and Bar-Joseph, 2006) based on the FPKM values. The hierarchical clustering of the gene sets was determined via Morpheus (<https://software.broadinstitute.org/morpheus/>) with one minus Pearson correlation as the distance metric and average as the linkage method based on the \log_2 (FPKM + 1) value. The gene coexpression networks were constructed via the WGCNA (v 1.63) package in R (Langfelder and Horvath, 2008). A total of 16 932 genes with an average FPKM of more than 1 from 24 samples were used to perform the coexpression network analysis by WGCNA. The automatic network construction function blockwiseModules was used to obtain the modules with default settings, except the maxBlockSize was set to 17 000, the minModuleSize was set to 30, and the power was set to 28. A

total of 11 844 genes were clustered into 15 tissue-specific modules, and 5088 genes were outliers (grey module). The eigengene value was calculated for each module and used to test the association with the phytohormone data. Cytoscape (V3.2.1) was used to visualize the networks (Shannon *et al.*, 2003).

Quantification of plant hormones

The samples used for the ABA, JA and IAA quantification were prepared according to the method described by Pan *et al.* (2010) with a few modifications. In brief, 200 mg of powdered fresh sample was transferred to a 10 mL screw-cap tube. A total of 50 μL working solution of internal standards and 2 mL extraction solvent, 2-propanol/ H_2O /concentrated HCl (2:1:0.002, vol/vol/vol), were added to each tube. The tubes were shaken for 30 min at 4°C and 200 rpm. Dichloromethane (4 mL) was added to each sample, and the samples were continually shaken for 30 min at 4°C . Then, the samples were centrifuged for 5 min at 13 000g and 4°C . A total of 4 mL of the solvent was transferred from the lower phase into a screw-cap vial, and the solvent mixture was concentrated using nitrogen flow. The samples were redissolved in 0.2 mL methanol and filtered with 0.22 μm organic membrane filters. The extracted solution was injected into the reverse-phase column (C₁₈ Gemini 5 μ , 150×2.00 mm) for a HPLC–ESI–MS/MS (ABI 4000 QTRAP, Applied Biosystems) analysis. The internal standard working solutions included d₆-ABA (Icon Isotopes, cat. no. ID1001), d₅-IAA (Aldrich, cat. no. 492817), and H₂JA (dihydrojasmonic acid, OlChemim, cat. no. 0145324) as the internal standards for ABA, IAA and JA, respectively. Each sample was characterized based on three replicates.

Measurement of physiological data

Approximately 0.5 g of peel material was used to determine the total chlorophyll content according to the method described by Li (2000). Each sample was assayed with three replicates. The colour index (CI) of the fruit peel was measured using the CIELAB colour system (CR-400, MINOLTA) according to the method described by Zhang *et al.* (2015). The gas chromatography (GC) method was used to determine the soluble sugar and organic acid concentrations of the fruit pulps as described previously (Yu *et al.*, 2012). The total soluble sugars (TSS) and total acid (TA) of the fruit pulps were measured by a portable refractometer (PAL-1, ATAGO) and an automatic potentiometric titrator (916Ti-Touch, Metrohm).

Hormonal treatment of citrus trees

A small-molecule ABA mimic, AM1 (Cao *et al.*, 2013), was used to treat the Satsuma mandarin (*Citrus unshiu*) trees. A total of 12 trees of equal vigour were selected for this experiment. A stock solution of 100 mM AM1 was made with DMSO and diluted with water before application. We set up three treatment concentrations (500, 800 and 1500 μM). The control group was treated with water. Each group consisted of three trees. One litre of solution was instilled into the main stem of the trees, which was expended in approximately three days. The treatments were administered at 135 and 175 DAF after samples collection. And the 135 DAF was set as control stage. The fruit samples were collected at 135, 160, 175 and 195 DAF.

Quantitative analysis of gene expression

The gene expression analysis via qRT-PCR was performed with three biological replicates in the QuantStudio™ 6 Flex real-time PCR system (Applied Biosystems) according to the method described in our previous study (Wu *et al.*, 2014b), and *CsActin*

was used as the endogenous reference gene (Wu *et al.*, 2014a). The primers are listed in Table S12.

Fluorescence *in situ* hybridization (FISH) assay

Three specific sequences of *SWEET15* (Cs7g02970) were used as templates to synthesize three specific fluorescent oligonucleotide probes (5'-GCTTCCAGTCTCTGCCTTATCTGGTAGCATTGTTTCAG CTC-3', 5'-AGCTTCTGAAGTGGACCCGGTTGTAATTCATCCTGA GTAT-3' and 5'-GCTTAGAAGTTCCTAGTGGTCTCCAGCTGCAG-CAGCATAA-3'). For *in situ* hybridization, JS slices (sampled at 150 DAF from *C. sinensis* fruit) were made and processed as described by Sunde *et al.* (2003).

Yeast one-hybrid assays

The promoter fragments containing ABRE *cis*-elements (CACGTG or ACGTG) were amplified by PCR using specific primers (Table S12). The amplified promoter fragments were cloned into pAbAi vector as the baits, and the full-length CDS of *CsABF2* was fused at the C terminus of GAL4-AD in the pGADT7 vector to construct the prey. Y1H assays were performed using the Matchmaker Gold Y1H Library Screening System (Clontech, Mountain View, CA) according to the manufacturer's protocol. The bait plasmids were transferred into Y1H yeast and screened for resistance concentrations using SD/-ura with different concentrations of aureobasidin A (AbA). The protein-DNA interaction was determined based on growth ability of the cotransformed yeast cells on SD/-Ura/Leu medium supplemented with the corresponding concentration of AbA.

Dual-luciferase assays

The full-length CDS of *CsABF2* was ligated to the pGreenII-62-SK-LUC vector, and the promoter fragments amplified by PCR using specific primers (Table S12) were ligated to the pGreenII-0800-LUC vector. Subsequently, the two recombinant plasmids were cotransferred into GV3101 (pSoup-p19). The pGreenII-62-SK-LUC vector without the *CsABF2* gene was used as a negative control. Activated *Agrobacterium* was used to infect tobacco (*Nicotiana benthamiana*) leaves, and the experimental group and the negative control were injected into the same tobacco leaf, with 4–5 leaves used per gene. Subsequently, the tobacco plants were cultured in a dark environment of 25 °C for 24 h, and then cultured for 3 days in an environment of 25 °C under light for 16 h and 22 °C under darkness for 8 h. LUC assays were measured using the Dual-Luciferase® Reporter Assay System (Promega) according to the manufacturer's instructions.

Acknowledgements

This research was supported by the National Key Research and Development Project (2019YFD1001400), Natural Science Foundation of China (NSFC) (32072541 31601729) and National Modern Citrus Industry System (CARS-26).

Conflicts of interest

The authors declare that they have no conflicts of interest.

Author contributions

H.Y. and J.W. conceived the project and designed the research. G.F., Y.X. and L.L. carried out samples collection and field experiments. J.W. and G.F. performed the bioinformatics analysis.

G.F. performed most of the experiments. J.W., G.F. and H.Y. wrote the paper. All authors read and approved the manuscript.

References

- Alexander, L. and Grierson, D. (2002) Ethylene biosynthesis and action in tomato: a model for climacteric fruit ripening. *J. Exp. Bot.* **53**, 2039–2055.
- Alferez, F. and Zacarias, L. (1999) Interaction between ethylene and abscisic acid in the regulation of citrus fruit maturation. In *Biology and Biotechnology of the Plant Hormone Ethylene II*. (Kanellis, A.K., Chang, C., Klee, H., Bleecker, A.B., Pech, J.C. and Grierson, D., eds), pp. 183–184. Dordrecht: Springer, Netherlands.
- Aluri, S. and Buttner, M. (2007) Identification and functional expression of the *Arabidopsis thaliana* vacuolar glucose transporter 1 and its role in seed germination and flowering. *Proc. Natl Acad. Sci. USA*, **104**, 2537–2542.
- Aoki, N., Hirose, T., Scofield, G.N., Whitfield, P.R. and Furbank, R.T. (2003) The sucrose transporter gene family in rice. *Plant Cell Physiol.* **44**, 223–232.
- Aprile, A., Federici, C., Close, T.J., De Bellis, L., Cattivelli, L. and Roose, M.L. (2011) Expression of the Hplus-ATPase AHA10 proton pump is associated with citric acid accumulation in lemon juice sac cells. *Funct. Integr. Genomic*, **11**, 551–563.
- Archbold, D. and Dennis, F. Jr. (1984) Quantification of free ABA and free and conjugated IAA in strawberry achene and receptacle tissue during fruit development. *J. Am. Soc. Hortic. Sci.* **109**, 330–335.
- Bain, J. (1958) Morphological, anatomical, and physiological changes in the developing fruit of the Valencia orange, *Citrus sinensis* (L) Osbeck. *Australian J. Bot.* **6**, 1–23.
- Berli, F.J., Fanzone, M., Piccoli, P. and Bottini, R. (2011) Solar UV-B and ABA are involved in phenol metabolism of *Vitis vinifera* L. increasing biosynthesis of berry skin polyphenols. *J. Agric. Food Chem.* **59**, 4874–4884.
- Brummell, D.A., Harpster, M.H. and Dunsmuir, P. (1999) Differential expression of expansin gene family members during growth and ripening of tomato fruit. *Plant Mol. Biol.* **39**, 161–169.
- Brune, A., Muller, M., Taiz, L., Gonzalez, P. and Etxeberria, E. (2002) Vacuolar acidification in citrus fruit: Comparison between acid lime (*Citrus aurantifolia*) and sweet lime (*Citrus limmetioides*) juice cells. *J. Am. Soc. Hortic. Sci.* **127**, 171–177.
- Cao, M.J., Liu, X., Zhang, Y., Xue, X.Q., Zhou, X.E., Melcher, K., Gao, P. *et al.* (2013) An ABA-mimicking ligand that reduces water loss and promotes drought resistance in plants. *Cell Res.* **23**, 1043–1054.
- Cercos, M., Soler, G., Iglesias, D.J., Gadea, J., Forment, J. and Talon, M. (2006a) Global analysis of gene expression during development and ripening of citrus fruit flesh. A proposed mechanism for citric Acid utilization. *Plant Mol. Biol.* **62**, 513–527.
- Cercos, M., Soler, G., Iglesias, D.J., Gadea, J., Forment, J. and Talon, M. (2006b) Global analysis of gene expression during development and ripening of citrus fruit flesh. A proposed mechanism for citric acid utilization. *Plant Mol. Biol.* **62**, 513–527.
- Chen, L.Q., Lin, I.W.N., Qu, X.Q., Sosso, D., McFarlane, H.E., Londono, A., Samuels, A.L. *et al.* (2015) A cascade of sequentially expressed sucrose transporters in the seed coat and endosperm provides nutrition for the *Arabidopsis* embryo. *Plant Cell*, **27**, 607–619.
- Chen, L.Q., Qu, X.Q., Hou, B.H., Sosso, D., Osorio, S., Fernie, A.R. and Frommer, W.B. (2012) Sucrose efflux mediated by SWEET proteins as a key step for phloem transport. *Science*, **335**, 207–211.
- D'Aoust, M.A., Yelle, S. and Nguyen-Quoc, B. (1999) Antisense inhibition of tomato fruit sucrose synthase decreases fruit setting and the sucrose unloading capacity of young fruit. *Plant Cell*, **11**, 2407–2418.
- Degu, A., Hatw, B., Nunes-Nesi, A., Shlizerman, L., Zur, N., Katz, E., Fernie, A.R. *et al.* (2011) Inhibition of aconitase in citrus fruit callus results in a metabolic shift towards amino acid biosynthesis. *Planta*, **234**, 501–513.
- Ding, Y.D., Chang, J.W., Ma, Q.L., Chen, L.L., Liu, S.Z., Jin, S., Han, J.W. *et al.* (2015) Network analysis of postharvest senescence process in citrus fruits revealed by transcriptomic and metabolomic profiling. *Plant Physiol.* **168**, 357–U642.
- Ernst, J. and Bar-Joseph, Z. (2006) STEM: a tool for the analysis of short time series gene expression data. *BMC Bioinform.* **7**, 191.
- Fan, J., Wang, H., Li, X., Sui, X. and Zhang, Z. (2019) Down-Regulating Cucumber Sucrose Synthase 4 (*CsSUS4*) suppresses the growth and development of flowers and fruits. *Plant Cell Physiol.* **60**, 752–764.

- Feng, G., Wu, J. and Yi, H. (2019) Global tissue-specific transcriptome analysis of *Citrus sinensis* fruit across six developmental stages. *Scientific Data*, **6**, 153.
- Goetz, M., Hooper, L.C., Johnson, S.D., Rodrigues, J.C., Vivian-Smith, A. and Koltunow, A.M. (2007) Expression of aberrant forms of AUXIN RESPONSE FACTOR8 stimulates parthenocarp in *Arabidopsis* and tomato. *Plant Physiol.* **145**, 351–366.
- Goldschmidt, E. (1998) Ripening of citrus and other non-climacteric fruits: A role for ethylene. *Acta Hort.* **463**, 335–340.
- Guo, L.X., Shi, C.Y., Liu, X., Ning, D.Y., Jing, L.F., Yang, H. and Liu, Y.Z. (2016) Citrate accumulation-related gene expression and/or enzyme activity analysis combined with metabolomics provide a novel insight for an orange mutant. *Sci. Rep.-UK*, **6**, 29343.
- Hollender, C.A., Kang, C.Y., Darwish, O., Geretz, A., Matthews, B.F., Slovin, J., Alkharouf, N. et al. (2014) Floral transcriptomes in woodland strawberry uncover developing receptacle and anther gene networks. *Plant Physiol.* **165**, 1062–1075.
- Hu, X.M., Shi, C.Y., Liu, X., Jin, L.F., Liu, Y.Z. and Peng, S.A. (2015) Genome-wide identification of citrus ATP-citrate lyase genes and their transcript analysis in fruits reveals their possible role in citrate utilization. *Mol. Genet. Genom.* **290**, 29–38.
- Huang, D.Q., Zhao, Y.H., Cao, M.H., Qiao, L. and Zheng, Z.L. (2016) Integrated systems biology analysis of transcriptomes reveals candidate genes for acidity control in developing fruits of sweet orange (*Citrus sinensis* L. Osbeck). *Front. Plant Sci.* **7**, 486.
- Hussain, S.B., Shi, C.Y., Guo, L.X., Kamran, H.M., Sadka, A. and Liu, Y.Z. (2017) Recent advances in the regulation of citric acid metabolism in citrus fruit. *Crit. Rev. Plant Sci.* **36**, 241–256.
- Islam, M.Z., Jin, L.-F., Shi, C.-Y., Liu, Y.-Z. and Peng, S.-A. (2015) Citrus sucrose transporter genes: genome-wide identification and transcript analysis in ripening and ABA-injected fruits. *Tree Genet. Genom.* **11**, 97.
- Ji, K., Chen, P., Sun, L., Wang, Y., Dai, S., Li, Q., Li, P. et al. (2012) Non-climacteric ripening in strawberry fruit is linked to ABA, FaNCED2 and FaCYP707A1. *Funct. Plant Biol.* **39**, 351–357.
- Jia, H.F., Chai, Y.M., Li, C.L., Lu, D., Luo, J.J., Qin, L. and Shen, Y.Y. (2011) Abscisic acid plays an important role in the regulation of strawberry fruit ripening. *Plant Physiol.* **157**, 188–199.
- Jia, H.F., Lu, D., Sun, J.H., Li, C.L., Xing, Y., Qin, L. and Shen, Y.Y. (2013) Type 2C protein phosphatase AB1 is a negative regulator of strawberry fruit ripening. *J. Exp. Bot.* 1677–1687.
- de Jong, M., Wolters-Arts, M., Feron, R., Mariani, C. and Vriezen, W.H. (2009) The *Solanum lycopersicum* auxin response factor 7 (SlARF7) regulates auxin signaling during tomato fruit set and development. *Plant J.* **57**, 160–170.
- Kachanovsky, D.E., Filler, S., Isaacson, T. and Hirschberg, J. (2012) Epistasis in tomato color mutations involves regulation of phytoene synthase 1 expression by cis-carotenoids. *Proc. Natl. Acad. Sci. USA*, **109**, 19021–19026.
- Kang, C.Y., Darwish, O., Geretz, A., Shahan, R., Alkharouf, N. and Liu, Z.C. (2013) Genome-scale transcriptomic insights into early-stage fruit development in woodland strawberry *Fragaria vesca*. *Plant Cell*, **25**, 1960–1978.
- Karlova, R., Chapman, N., David, K., Angenent, G.C., Seymour, G.B. and de Maagd, R.A. (2014) Transcriptional control of fleshy fruit development and ripening. *J. Exp. Bot.* **65**, 4527–4541.
- Katz, E., Boo, K.H., Kim, H.Y., Eigenheer, R.A., Phinney, B.S., Shulaev, V., Negre-Zakharov, F. et al. (2011) Label-free shotgun proteomics and metabolite analysis reveal a significant metabolic shift during citrus fruit development. *J. Exp. Bot.* **62**, 5367–5384.
- Klee, H.J. and Giovannoni, J.J. (2011) Genetics and control of tomato fruit ripening and quality attributes. *Annu. Rev. Genet.* **45**, 41–59.
- Koch, K.E. (1983) The path of photosynthate translocation into citrus fruit. *Plant Physiol.* **72**, 69–69.
- Koch, K.E. and Avigne, W.T. (1990) Postphloem, nonvascular transfer in citrus - kinetics, metabolism, and sugar gradients. *Plant Physiol.* **93**, 1405–1416.
- Koch, K.E., Lowell, C.A. and Avigne, W.T. (1986) Assimilate transfer through citrus juice vesicle stalks: a nonvascular portion of the transport path. In *Plant Biology*, Vol. 1: Phloem Transport (Cronshaw, J., Lucas, W.T. and Giaquinta, R.T., eds), pp. 247–258. New York, NY: Alan Liss Inc.
- Kojima, K., Yamada, Y. and Yamamoto, M. (1995) Effects of abscisic-acid injection on sugar and organic-acid contents of citrus-fruit. *J. Jpn. Soc. Hortic. Sci.* **64**, 17–21.
- Langfelder, P. and Horvath, S. (2008) WGCNA: an R package for weighted correlation network analysis. *BMC Bioinform.* **9**, 559.
- Leng, P., Yuan, B. and Guo, Y. (2014) The role of abscisic acid in fruit ripening and responses to abiotic stress. *J. Exp. Bot.* **65**, 4577–4588.
- Li, H.S. (2000) *Principles and Techniques of Plant Physiology and Biochemistry Experiment*, pp. 134–137. Beijing: Higher Education Press.
- Li, X., Guo, W., Li, J., Yue, P., Bu, H., Jiang, J., Liu, W. et al. (2020) Histone acetylation at the promoter for the transcription factor PuWRKY31 affects sucrose accumulation in pear fruit. *Plant Physiol.* **182**(4), 2035–2046.
- Li, S.J., Yin, X.R., Wang, W.L., Liu, X.F., Zhang, B. and Chen, K.S. (2017) Citrus CitNAC62 cooperates with CitWRKY1 to participate in citric acid degradation via up-regulation of CitAco3. *J. Exp. Bot.* **68**, 3419–3426.
- Lin, Q., Li, S., Dong, W., Feng, C., Yin, X., Xu, C., Sun, C. et al. (2015a) Involvement of CitCHX and CitDIC in developmental-related and postharvest-hot-air driven citrate degradation in citrus fruits. *PLoS One*, **10**, e0119410.
- Lin, I.W., Sosso, D., Chen, L.Q., Gase, K., Kim, S.G., Kessler, D., Klinkenberg, P.M. et al. (2014) Nectar secretion requires sucrose phosphate synthases and the sugar transporter SWEET9. *Nature*, **508**, 546–549.
- Lin, Q., Wang, C., Dong, W., Jiang, Q., Wang, D., Li, S., Chen, M. et al. (2015b) Transcriptome and metabolome analyses of sugar and organic acid metabolism in Ponkan (*Citrus reticulata*) fruit during fruit maturation. *Gene*, **554**, 64–74.
- Liu, X., Hu, X.M., Jin, L.F., Shi, C.Y., Liu, Y.Z. and Peng, S.A. (2014) Identification and transcript analysis of two glutamate decarboxylase genes, CsGAD1 and CsGAD2, reveal the strong relationship between CsGAD1 and citrate utilization in citrus fruit. *Mol. Biol. Rep.* **41**, 6253–6262.
- Liu, Y., Liu, Q. and Tao, N. (2006) Efficient isolation of RNA from fruit peel and pulp of ripening navel orange (*Citrus sinensis* Osbeck). *J. Huazhong Agric. Univ.* **25**, 300–304.
- Ma, Q.J., Sun, M.H., Lu, J., Liu, Y.J., Hu, D.G. and Hao, Y.J. (2017) Transcription factor AREB2 is involved in soluble sugar accumulation by activating sugar transporter and amylase genes. *Plant Physiol.* **174**, 2348–2362.
- Muller, M.L., IrkensKiesecker, U., Rubinstein, B. and Taiz, L. (1996) On the mechanism of hyperacidification in lemon - Comparison of the vacuolar H⁺-ATPase activities of fruits and epicotyls. *J. Biol. Chem.* **271**, 1916–1924.
- Muller, M.L. and Taiz, L. (2002) Regulation of the lemon-fruit V-ATPase by variable stoichiometry and organic acids. *J. Membrane Biol.* **185**, 209–220.
- Nii, N. and Coombe, B. G. (1988) Anatomical aspects of juice sacs of satsuma mandarin in relation to translocation. *J. Jpn. Soc. Hortic. Sci.* **56**, 375–381.
- Pan, X., Welti, R. and Wang, X. (2010) Quantitative analysis of major plant hormones in crude plant extracts by high-performance liquid chromatography-mass spectrometry. *Nat. Protoc.* **5**, 986–992.
- Pattison, R.J., Csukasi, F. and Catala, C. (2014) Mechanisms regulating auxin action during fruit development. *Physiol. Plant.* **151**, 62–72.
- Pattison, R.J., Csukasi, F., Zheng, Y., Fei, Z., van der Knaap, E. and Catala, C. (2015) Comprehensive tissue-specific transcriptome analysis reveals distinct regulatory programs during early tomato fruit development. *Plant Physiol.* **168**, 1684–1701.
- Paul, V., Pandey, R. and Srivastava, G.C. (2012) The fading distinctions between classical patterns of ripening in climacteric and non-climacteric fruit and the ubiquity of ethylene-An overview. *J. Food Sci. Tech. Mys* **49**, 1–21.
- Payyavula, R.S., Tay, K.H., Tsai, C.J. and Harding, S.A. (2011) The sucrose transporter family in *Populus*: the importance of a tonoplast PtaSUT4 to biomass and carbon partitioning. *Plant J.* **65**, 757–770.
- Reuscher, S., Akiyama, M., Yasuda, T., Makino, H., Aoki, K., Shibata, D. and Shiratake, K. (2014) The sugar transporter inventory of tomato: genome-wide identification and expression analysis. *Plant Cell Physiol.* **55**, 1123–1141.
- Rodrigo, M.J., Marcos, J.F., Alf  rez, F., Mallent, M.D. and Zacar  as, L. (2003) Characterization of Pinalate, a novel *Citrus sinensis* mutant with a fruit-specific alteration that results in yellow pigmentation and decreased ABA content. *J. Exp. Bot.* **54**, 727–738.
- Romero, P., Lafuente, M.T. and Rodrigo, M.J. (2012) The Citrus ABA signalosome: identification and transcriptional regulation during sweet orange fruit ripening and leaf dehydration. *J. Exp. Bot.* **63**, 4931–4945.
- Sadka, A., Dahan, E., Cohen, L. and Marsh, K.B. (2000) Aconitase activity and expression during the development of lemon fruit. *Physiol. Plant.* **108**, 255–262.
- Sadka, A., Shlizerman, L., Kamara, I. and Blumwald, E. (2019) Primary metabolism in citrus fruit as affected by its unique structure. *Front. Plant Sci.* **10**, 1167.

- Schneider, S., Hulpke, S., Schulz, A., Yaron, I., Holl, J., Imlau, A., Schmitt, B. et al. (2012) Vacuoles release sucrose via tonoplast-localised SUC4-type transporters. *Plant Biol.* **14**, 325–336.
- Schulz, A., Beyhl, D., Marten, I., Wormit, A., Neuhaus, E., Poschet, G., Buttnar, M. et al. (2011) Proton-driven sucrose symport and antiport are provided by the vacuolar transporters SUC4 and TMT1/2. *Plant J.* **68**, 129–136.
- Shannon, P., Markiel, A., Ozier, O., Baliga, N.S., Wang, J.T., Ramage, D., Amin, N. et al. (2003) Cytoscape: A software environment for integrated models of biomolecular interaction networks. *Genome Res.* **13**, 2498–2504.
- Sheng, L., Shen, D., Yang, W., Zhang, M., Zeng, Y., Xu, J., Deng, X. et al. (2017) GABA pathway rate-limit citrate degradation in postharvest citrus fruit evidence from HB Pumelo (*Citrus grandis*) × Fairchild (*Citrus reticulata*) hybrid population. *J. Agric. Food Chem.* **65**, 1669–1676.
- Shi, C.Y., Hussain, S.B., Yang, H., Bai, Y.X., Khan, M.A. and Liu, Y.Z. (2019) CspH8, a P-type proton pump gene, plays a key role in the diversity of citric acid accumulation in citrus fruits. *Plant Sci.* **289**, 110288.
- Shi, C.Y., Song, R.Q., Hu, X.M., Liu, X., Jin, L.F. and Liu, Y.Z. (2015) Citrus PH5-like H⁺-ATPase genes: identification and transcript analysis to investigate their possible relationship with citrate accumulation in fruits. *Front. Plant Sci.* **6**, 135.
- Shimada, T., Nakano, R., Shulaev, V., Sadka, A. and Blumwald, E. (2006) Vacuolar citrate/H⁺ symporter of citrus juice cells. *Planta* **224**, 472–480.
- Shlizerman, L., Marsh, K., Blumwald, E. and Sadka, A. (2007) Iron-shortage-induced increase in citric acid content and reduction of cytosolic aconitase activity in Citrus fruit vesicles and calli. *Physiol. Plant*, **131**, 72–79.
- Staswick, P.E., Serban, B., Rowe, M., Tiryaki, I., Maldonado, M.T., Maldonado, M.C. and Suza, W. (2005) Characterization of an Arabidopsis enzyme family that conjugates amino acids to indole-3-acetic acid. *Plant Cell*, **17**, 616–627.
- Strazzer, P., Spelt, C.E., Li, S., Blik, M., Federici, C.T., Roose, M.L., Koes, R. et al. (2019) Hyperacidification of Citrus fruits by a vacuolar proton-pumping P-ATPase complex. *Nat. Commun.* **10**, 744.
- Sun, L., Sun, Y.F., Zhang, M., Wang, L., Ren, J., Cui, M.M., Wang, Y.P. et al. (2012a) Suppression of 9-cis-epoxycarotenoid dioxygenase, which encodes a key enzyme in abscisic acid biosynthesis, alters fruit texture in transgenic tomato. *Plant Physiol.* **158**, 283–298.
- Sun, L., Yuan, B., Zhang, M., Wang, L., Cui, M., Wang, Q. and Leng, P. (2012b) Fruit-specific RNAi-mediated suppression of SINCED1 increases both lycopene and β-carotene contents in tomato fruit. *J. Exp. Bot.* **63**, 3097–3108.
- Sundberg, E. and Ostergaard, L. (2009) Distinct and dynamic auxin activities during reproductive development. *Cold Spring Harbor Perspect. Biol.* **1**, a001628.
- Sunde, P.T., Olsen, I., Gobel, U.B., Theegarten, D., Winter, S., Debelian, G.J., Tronstad, L. et al. (2003) Fluorescence in situ hybridization (FISH) for direct visualization of bacteria in periapical lesions of asymptomatic root-filled teeth. *Microbiol-Sgm.* **149**, 1095–1102.
- Sundell, D., Street, N.R., Kumar, M., Mellerowicz, E.J., Kucukoglu, M., Johnsson, C., Kumar, V. et al. (2017) AspWood: high-spatial-resolution transcriptome profiles reveal uncharacterized modularity of wood formation in *Populus tremula*. *Plant Cell*, **29**, 1585.
- Tang, G.Q., Luscher, M. and Sturm, A. (1999) Antisense repression of vacuolar and cell wall invertase in transgenic carrot alters early plant development and sucrose partitioning. *Plant Cell*, **11**, 177–189.
- Wang, Y., Ji, K., Dai, S., Hu, Y., Sun, L., Li, Q., Chen, P. et al. (2013) The role of abscisic acid in regulating cucumber fruit development and ripening and its transcriptional regulation. *Plant Physiol. Biochem.* **64**, 70–79.
- Wang, Y., Wu, Y., Duan, C., Chen, P., Li, Q., Dai, S., Sun, L. et al. (2012) The expression profiling of the CsPYL, CsPP2C and CsSnRK2 gene families during fruit development and drought stress in cucumber. *J. Plant Physiol.* **169**, 1874–1882.
- Wang, X., Yin, W., Wu, J., Chai, L. and Yi, H. (2016) Effects of exogenous abscisic acid on the expression of citrus fruit ripening-related genes and fruit ripening. *Scientia Hort.* **201**, 175–183.
- Wu, J., Su, S., Fu, L., Zhang, Y., Chai, L. and Yi, H. (2014a) Selection of reliable reference genes for gene expression studies using quantitative real-time PCR in navel orange fruit development and pummelo floral organs. *Scientia Hort.* **176**, 180–188.
- Wu, J., Xu, Z., Zhang, Y., Chai, L., Yi, H. and Deng, X. (2014b) An integrative analysis of the transcriptome and proteome of the pulp of a spontaneous late-ripening sweet orange mutant and its wild type improves our understanding of fruit ripening in citrus. *J. Exp. Bot.* **65**, 1651–1671.
- Xu, Y., Tao, Y.Y., Cheung, L.S., Fan, C., Chen, L.Q., Xu, S., Perry, K. et al. (2014) Structures of bacterial homologues of SWEET transporters in two distinct conformations. *Nature*, **515**, 448–452.
- Yu, X., Wang, X., Zhang, W., Qian, T., Tang, G., Guo, Y. and Zheng, C. (2008) Antisense suppression of an acid invertase gene (MA11) in muskmelon alters plant growth and fruit development. *J. Exp. Bot.* **59**, 2969–2977.
- Yu, K., Xu, Q., Da, X., Guo, F., Ding, Y. and Deng, X. (2012) Transcriptome changes during fruit development and ripening of sweet orange (*Citrus sinensis*). *Bmc Genom.* **13**, 10.
- Zhan, J.P., Thakare, D., Ma, C., Lloyd, A., Nixon, N.M., Arakaki, A.M., Burnett, W.J. et al. (2015) RNA sequencing of laser-capture microdissected compartments of the maize kernel identifies regulatory modules associated with endosperm cell differentiation. *Plant Cell*, **27**, 513–531.
- Zhang, Y.-J., Wang, X.-J., Wu, J.-X., Chen, S.-Y., Chen, H., Chai, L.-J. and Yi, H.-L. (2015) Comparative transcriptome analyses between a spontaneous late-ripening sweet orange mutant and its wild type suggest the functions of ABA, sucrose and JA during citrus fruit ripening. *PLoS One*, **9**, e116056.
- Zhu, F., Luo, T., Liu, C., Wang, Y., Yang, H., Yang, W., Zheng, L. et al. (2017) An R2R3-MYB transcription factor represses the transformation of α- and β-branch carotenoids by negatively regulating expression of CrBCH2 and CrNCED5 in flavedo of Citrus reticulata. *New Phytol.* **216**, 178–192.

Supporting information

Additional supporting information may be found online in the Supporting Information section at the end of the article.

Figure S1 Visualization of the GO enrichment analysis of the genes in profiles 8 and 39 in the four fruit tissues by REVIGO.

Figure S2 Coexpression modules identified by WGCNA.

Figure S3 Correlation networks of the green (a) and yellow (b) modules.

Figure S4 Gene expression heatmap of *Expansins*.

Figure S5 Expression profiling of hormone-related genes and the contents of total carotenoids in the four fruit tissues at six developmental stages.

Figure S6 Sucrose metabolism-related genes.

Figure S7 Citric acid metabolism-related genes.

Figure S8 Content of soluble sugars and organic acids of treated Satsuma fruits.

Table S1 RNA-seq statistics.

Table S2 Gene expression in the four fruit tissues at six developmental stages.

Table S3 Data from the STEM analysis.

Table S4 GO term enrichment analysis of the genes in profiles 8 and 39 in the four fruit tissues.

Table S5 KEGG pathway enrichment analysis results of the genes in profiles 8 and 39 in the four fruit tissues.

Table S6 Data from the WGCNA analysis.

Table S7 GO term enrichment analysis results of the black, blue, purple, green, yellow and brown modules.

Table S8 Module network file for the blue, black, purple, green and yellow modules.

Table S9 Number of *cis*-elements in the promotor of *Expansin* genes.

Table S10 List of key genes identified by RNA-seq.

Table S11 Statistically significant difference analysis of the content of ABA, IAA and JA among different stages and tissues.

Table S12 Primers used in this study.